

# Higher Charmonia

T.Barnes,<sup>a\*</sup> S.Godfrey<sup>b†</sup> and E.S.Swanson<sup>c‡</sup>

<sup>a</sup>*Department of Physics and Astronomy,  
University of Tennessee, Knoxville, TN 37996, USA,  
Physics Division, Oak Ridge National Laboratory,  
Oak Ridge, TN 37831, USA*

<sup>b</sup>*Ottawa-Carleton Institute for Physics,  
Department of Physics, Carleton University,  
Ottawa K1S 5B6, Canada*

<sup>c</sup>*Rudolph Peierls Centre for Theoretical Physics,  
Oxford University, Oxford, OX1 3NP, UK.*

(Dated: November 26, 2024)

This paper gives results for the spectrum, all allowed E1 radiative partial widths (and some important M1 widths) and all open-charm strong decay amplitudes of all 40  $c\bar{c}$  states expected up to the mass of the 4S multiplet, just above 4.4 GeV. The spectrum and radiative widths are evaluated using two models, the relativized Godfrey-Isgur model and a nonrelativistic potential model. The electromagnetic transitions are evaluated using Coulomb plus linear plus smeared hyperfine wavefunctions, both in a nonrelativistic potential model and in the Godfrey-Isgur model. The open-flavor strong decay amplitudes are determined assuming harmonic oscillator wavefunctions and the  $^3P_0$  decay model. This work is intended to motivate future experimental studies of higher-mass charmonia, and may be useful for the analysis of high-statistics data sets to be accumulated by the BES, CLEO and GSI facilities.

PACS numbers: 12.39.-x, 13.20.Gd, 13.25.Gv, 14.40.Gx

## I. INTRODUCTION

Since its discovery in 1974 [1, 2], the charmonium system has become the prototypical ‘hydrogen atom’ of meson spectroscopy [3, 4, 5, 6]. The experimentally clear spectrum of relatively narrow states below the open-charm DD threshold of 3.73 GeV can be identified with the 1S, 1P and 2S  $c\bar{c}$  levels predicted by potential models, which incorporate a color Coulomb term at short distances and a linear scalar confining term at large distances. Spin-dependent interquark forces are evident in the splittings of states within these multiplets, and the observed splittings are consistent with the predictions of a one gluon exchange (OGE) Breit-Fermi Hamiltonian, combined with a linear scalar confining interaction. Discussions of the theoretical importance and experimental status of heavy quarkonium, including recent experimental results for charmonium, have been given by Quigg [7], Galik [8], the CERN quarkonium working group [9], Seth [10, 11, 12] and Swarnicki [13].

Recently there has been a resurgence of interest in charmonium, due to the realization that B factories can contribute to the study of the missing  $c\bar{c}$  states [14], and to high-statistics experiments at BES [15] and CLEO [16] and the planned GSI  $p\bar{p}$  facility [17].

The possibility of contributions from B factories was dramatically illustrated by the recent discovery of the long missing  $2^1S_0 \eta'_c$  state by the Belle Collaboration [18], which has since been confirmed by BABAR [19], and has also been observed by CLEO in  $\gamma\gamma$  collisions [20].

Additional interest in  $c\bar{c}$  spectroscopy has followed the discovery of the remarkable X(3872) by Belle [21] and CDF [22] in B decays to  $J/\psi\pi^+\pi^-$ ; assuming that this is a real resonance rather than a threshold effect, the X(3872) is presumably either a DD\* charmed meson molecule [23, 24, 25] or a narrow  $J = 2$  D-wave  $c\bar{c}$  state [26, 27]. Very recent observations of the X(3872) in  $\gamma J/\psi$  and  $\omega J/\psi$  by Belle support a  $1^{++}$  DD\* molecule assignment [28, 29].

There has also been experimental activity in the spin-singlet P-wave sector, with recent reports of the observation of the elusive  $1^1P_1 h_c$  state by CLEO [10, 30]. Finally, the surprisingly large cross sections for double charmonium production in  $e^+e^-$  reported by Belle [31, 32, 33, 34] suggest that it may be possible to study  $C = (+)$   $c\bar{c}$  states in  $e^+e^-$  without using the higher-order  $O(\alpha^4)$  two-photon annihilation process.

One open topic of great current interest in  $c\bar{c}$  spectroscopy is the search for the  $\psi_2(1^3D_2)$  and  $\eta_{c2}(1^1D_2)$  states, which are expected to be quite narrow due to the absence of open-charm decay modes.

A second topic is the Lorentz nature of confinement; in pure  $c\bar{c}$  models this is tested by the multiplet splittings of orbitally-excited  $c\bar{c}$  states. For example, with pure scalar confinement as is normally assumed there is no spin-spin hyperfine interaction at  $O(v^2/c^2)$ , so the masses of spin-singlets (such as the  $1^1P_1 h_c$ ) are degenerate with the corresponding triplet c.o.g. (center of gravity); here this

---

\*Email: tbarnes@utk.edu

†Email: godfrey@physics.carleton.ca

‡On leave from the Department of Physics and Astronomy, University of Pittsburgh, Pittsburgh PA 15260. Email: swansone@pitt.edu

is the  ${}^3P_J$  c.o.g., at 3525 MeV. In the original Cornell model [35] it was assumed that confinement acts as the time component of a Lorentz vector, which lifts the degeneracy of the  $h_c$  and the  ${}^3P_J$  c.o.g. Another possibility is that confinement may be a more complicated mix of scalar and timelike vector [36]. Of course these simple potential model considerations may be complicated by mass shifts due to other effects, such as couplings to open-flavor channels [27].

A third topic is the search for exotica such as hybrids; the level of mixing between conventional quarkonium and hybrid basis states falls rapidly with increasing quark mass, which suggests that nonexotic hybrids may be more easily distinguished from conventional quarkonia in charmonium than in the light quark sectors. Since LGT (lattice gauge theory) predicts that the lightest  $c\bar{c}$  hybrids lie near 4.4 GeV [37, 38, 39, 40], there is a strong incentive to establish the “background” spectrum of conventional  $c\bar{c}$  states up to and somewhat beyond this mass.

A final topic of current interest is the importance of mixing between quark model  $q\bar{q}$  basis states and two-meson continua, which has been cited as a possible reason for the low masses of the recently discovered  $D_{sJ}$  states [41, 42]. The effects of “unquenching the quark model” by including meson loops can presumably be studied effectively in the  $c\bar{c}$  system, in which the experimental spectrum of states is relatively unambiguous. The success of the  $q\bar{q}$  quark model is surprising, in view of the probable importance of corrections to the valence approximation; the range of validity of the naive “quenched”  $q\bar{q}$  quark model is an interesting and open question [43].

Motivated by this revived interest in  $c\bar{c}$  spectroscopy, we have carried out a theoretical study of the expected properties of charmonium states, notably the poorly understood higher-mass  $c\bar{c}$  levels above DD threshold. Two variants of potential models are used in this study, a conventional nonrelativistic model based on the Schrödinger equation with a Coulomb plus linear potential, and the Godfrey-Isgur relativized potential model. We give results for all states in the multiplets 1-4S, 1-3P, 1-2D, 1-2F and 1G, comprising 40  $c\bar{c}$  resonances in total. Predictions are given for quantities which are likely to be of greatest experimental interest, which are the spectrum of states, E1 (and some M1) electromagnetic transition rates, and strong partial and total widths of states above open-charm threshold.

Similar results for many of the electromagnetic transition rates have recently been reported by Ebert *et al.* [44]. The  $\ell^+\ell^-$  leptonic and two-photon widths are not discussed in detail here, as they have been considered extensively elsewhere; see for example [45] and [46, 47, 48] and references cited therein.

## II. SPECTRUM

### A. Nonrelativistic potential model

As a minimal model of the charmonium system we use a nonrelativistic potential model, with wavefunctions determined by the Schrödinger equation with a conventional quarkonium potential. We use the standard color Coulomb plus linear scalar form, and also include a Gaussian-smearred contact hyperfine interaction in the zeroth-order potential. The central potential is

$$V_0^{(c\bar{c})}(r) = -\frac{4}{3}\frac{\alpha_s}{r} + br + \frac{32\pi\alpha_s}{9m_c^2}\tilde{\delta}_\sigma(r)\vec{S}_c \cdot \vec{S}_{\bar{c}} \quad (1)$$

where  $\tilde{\delta}_\sigma(r) = (\sigma/\sqrt{\pi})^3 e^{-\sigma^2 r^2}$ . The four parameters  $(\alpha_s, b, m_c, \sigma)$  are determined by fitting the spectrum.

The spin-spin contact hyperfine interaction is one of the spin-dependent terms predicted by one gluon exchange (OGE) forces. The contact form  $\propto \delta(\vec{x})$  is actually an artifact of an  $O(v_q^2/c^2)$  expansion of the T-matrix [49], so replacing it by an interaction with a range  $1/\sigma$  comparable to  $1/m_c$  is not an unwarranted modification.

We treat the remaining spin-dependent terms as mass shifts using leading-order perturbation theory. These are the OGE spin-orbit and tensor and a longer-ranged inverted spin-orbit term, which arises from the assumed Lorentz scalar confinement. These are explicitly

$$V_{spin-dep} = \frac{1}{m_c^2} \left[ \left( \frac{2\alpha_s}{r^3} - \frac{b}{2r} \right) \vec{L} \cdot \vec{S} + \frac{4\alpha_s}{r^3} T \right]. \quad (2)$$

The spin-orbit operator is diagonal in a  $|J, L, S\rangle$  basis, with the matrix elements  $\langle \vec{L} \cdot \vec{S} \rangle = [J(J+1) - L(L+1) - S(S+1)]/2$ . The tensor operator T has nonvanishing diagonal matrix elements only between  $L > 0$  spin-triplet states, which are

$$\langle {}^3L_J | T | {}^3L_J \rangle = \begin{cases} -\frac{L}{6(2L+3)}, & J = L + 1 \\ +\frac{1}{6}, & J = L \\ -\frac{(L+1)}{6(2L-1)}, & J = L - 1 \end{cases}. \quad (3)$$

For experimental input we use the masses of the 11 reasonably well established  $c\bar{c}$  states, which are given in Table I (rounded to 1 MeV). The parameters that follow from fitting these masses are  $(\alpha_s, b, m_c, \sigma) = (0.5461, 0.1425 \text{ GeV}^2, 1.4794 \text{ GeV}, 1.0946 \text{ GeV})$ . Given these values, we can predict the masses and matrix elements of the currently unknown  $c\bar{c}$  states; Table I and Fig. 1 show the predicted spectrum.

### B. Godfrey-Isgur relativized potential model

The Godfrey-Isgur model is a “relativized” extension of the nonrelativistic model of the previous section. This

model assumes a relativistic dispersion relation for the quark kinetic energy, a QCD-motivated running coupling  $\alpha_s(r)$ , a flavor-dependent potential smearing parameter  $\sigma$ , and replaces factors of quark mass with quark kinetic energy. Details of the model and the method of solution may be found in Ref.[50]. The Hamiltonian consists of a relativistic kinetic term and a generalized quark-antiquark potential,

$$H = H_0 + V_{q\bar{q}}(\vec{p}, \vec{r}) \quad (4)$$

where

$$H_0 = \sqrt{\vec{p}_q^2 + m_q^2} + \sqrt{\vec{p}_{\bar{q}}^2 + m_{\bar{q}}^2}. \quad (5)$$

Just as in the nonrelativistic model, the quark-antiquark potential  $V_{q\bar{q}}(\vec{p}, \vec{r})$  assumed here incorporates the Lorentz vector one gluon exchange interaction at short distances and a Lorentz scalar linear confining interaction. To first order in  $(v_q/c)^2$ ,  $V_{q\bar{q}}(\vec{p}, \vec{r})$  reduces to the standard non-relativistic result given by Eqns.(1) and (2) (with  $\alpha_s$  replaced by a running coupling constant,  $\alpha_s(r)$ ). The full set of model parameters is given in Ref.[50]. Note that the string tension and quark mass ( $b = 0.18 \text{ GeV}^2$  and  $m_c = 1.628 \text{ GeV}$ ) are significantly larger than the values used in our nonrelativistic model.

One important aspect of this model is that it gives reasonably accurate results for the spectrum and matrix elements of quarkonia of all  $u, d, s, c, b$  quark flavors, whereas the nonrelativistic model of the previous section is only fitted to the  $c\bar{c}$  system.

### C. Discussion

The spectra predicted by the NR and GI models (Table I and Fig. 1) are quite similar for S- and P-wave states, largely because of the constraints provided by the experimental  $c\bar{c}$  candidates for these multiplets. We note in passing that these potential model results are very similar to the most recent predictions of the charmonium spectrum from LGT [38, 51, 52]. At higher L we have only the L=2  $1^3D_1$  and  $2^3D_1$  states  $\psi(3770)$  and  $\psi(4159)$  to constrain the models, and the predicted mean D-wave multiplet masses differ by *ca.* 50 MeV. For  $L > 2$  the absence of experimental states allows a relatively large scatter of predicted mean masses, which differ by as much as  $\approx 100 \text{ MeV}$  in the 1G multiplet. (The splittings within higher L multiplets in contrast are rather similar.) The mean multiplet masses predicted by the two models differ largely because of the values assumed for the string tension  $b$ , which is  $0.18 \text{ GeV}^2$  in the GI model but is a rather smaller  $0.1425 \text{ GeV}^2$  in the NR model. Identification of any L=3 or L=4  $c\bar{c}$  state would be very useful as

a constraint on the spectrum of higher-L  $c\bar{c}$  states generally. This is unfortunately a difficult problem, since these states are not easily accessible experimentally. As we shall see, one possibility is to produce the  $^3F_2 \chi_2 c\bar{c}$  state, which is formed in E1 radiative transitions from the  $\psi(4159)$  and decays dominantly to DD and DD\*. (For simplicity in this paper we abbreviate the final state DD as “DD”, the state  $DD^* + \bar{D}D^*$  as “DD\*”, and so forth.)

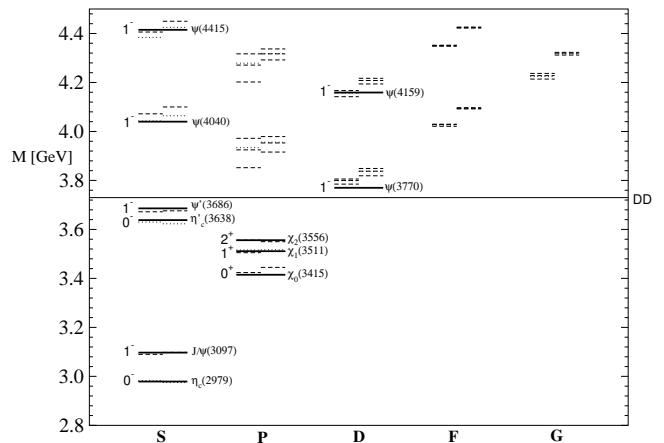


FIG. 1: Predicted and observed spectrum of charmonium states (Table I). The solid lines are experiment, and the broken lines are theory (NR model left, GI right). Spin triplet levels are dashed, and spin singlets are dotted. The DD open-charm threshold at 3.73 GeV is also shown.

## III. RADIATIVE TRANSITIONS

### A. E1 transitions

Radiative transitions of higher-mass charmonium states are of interest largely because they provide one of the few pathways between  $c\bar{c}$  states with different quantum numbers. Since typical E1 radiative partial widths of charmonia are 10s to 100s of keV, corresponding to significant branching fractions of  $\sim 10^{-3}$  to  $10^{-2}$ , large event samples of radially excited S-wave states produced in  $e^+e^-$  annihilation could be used to identify radially excited P-wave states, which are not otherwise easily produced. Similarly, the E1 radiative transition of the nominally  $2^3D_1 \psi(4159)$  can be used to produce an F-wave  $c\bar{c}$  state; this multiplet would likely be very difficult to reach using other mechanisms.

We evaluate these E1 radiative partial widths using

$$\Gamma_{\text{E1}}(n^{2S+1}L_J \rightarrow n'^{2S'+1}L'_{J'} + \gamma) = \frac{4}{3} C_{fi} \delta_{SS'} e_c^2 \alpha |\langle \psi_f | r | \psi_i \rangle|^2 E_\gamma^3 \frac{E_f^{(c\bar{c})}}{M_i^{(c\bar{c})}}, \quad (6)$$

where  $e_c = 2/3$  is the  $c$ -quark charge in units of  $|e|$ ,  $\alpha$  is the fine-structure constant,  $E_\gamma$  is the final photon energy,  $E_f^{(c\bar{c})}$  is the total energy of the final  $c\bar{c}$  state,  $M_i^{(c\bar{c})}$  is the mass of the initial  $c\bar{c}$  state, the spatial matrix element  $\langle \psi_f | r | \psi_i \rangle$  involves the initial and final radial wavefunctions, and the angular matrix element  $C_{fi}$  is

$$C_{fi} = \max(L, L') (2J' + 1) \begin{Bmatrix} L' & J' & S \\ J & L & 1 \end{Bmatrix}^2. \quad (7)$$

This is the result of Ref.[53], except for our inclusion of the relativistic phase space factor of  $E_f^{(c\bar{c})}/M_i^{(c\bar{c})}$ , which is usually not far from unity. (The GI results do not include this phase space factor.) We evaluate these radiative partial widths in both the NR and GI models. For the NR model the matrix elements  $\langle n'^{2S'+1}L'_{J'} | r | n^{2S+1}L_J \rangle$  were evaluated using the Coulomb plus linear plus smeared hyperfine wavefunctions of the potential model described in Sec.IIA, and for the GI model they were evaluated using the wavefunctions of Ref.[50]. Since the masses predicted for unknown states differ in the two models, the assumed photon energy  $E_\gamma$  differs as well; these photon energies are given in the E1 and M1 transition tables (Tables II-IX) together with the radiative partial widths.

Some E1 transitions that are of special importance for

the study of higher charmonium states are discussed in the text. Transitions from initial  $1^{--}$   $c\bar{c}$  states are of greatest interest in this regard, since these can be studied with high statistics at  $e^+e^-$  machines. These can provide access to the spin-triplet members of the 2P and 3P multiplets in particular, starting from the  $\psi(4040)$  and  $\psi(4415)$ . E1 radiative transitions may also be useful in identifying the narrow 1D  $3^-$  and  $2^-$   $c\bar{c}$  states, since they are all predicted to have large partial widths (*ca.* 300 keV) to the 1P  $\chi_J$  and  $h_c$  states.

## B. M1 transitions

Although M1 rates are typically rather weaker than E1 rates, they are nonetheless interesting because they may allow access to spin-singlet states that are very difficult to produce otherwise. It is also interesting that the known M1 rates show serious disagreement between theory and experiment. This is in part due to the fact that M1 transitions between different spatial multiplets, such as  $\psi' \rightarrow \gamma\eta_c$  ( $2S \rightarrow 1S$ ), are nonzero only due to small relativistic corrections to a vanishing lowest-order M1 matrix element.

The M1 radiative partial widths are evaluated using

$$\Gamma_{\text{M1}}(n^{2S+1}L_J \rightarrow n'^{2S'+1}L'_{J'} + \gamma) = \frac{4}{3} \frac{2J' + 1}{2L + 1} \delta_{LL'} \delta_{S,S' \pm 1} e_c^2 \frac{\alpha}{m_c^2} |\langle \psi_f | \psi_i \rangle|^2 E_\gamma^3 \frac{E_f^{(c\bar{c})}}{M_i^{(c\bar{c})}}. \quad (8)$$

(See the previous E1 formula for definitions.) The GI M1 radiative rates do not incorporate the  $E_f^{(c\bar{c})}/M_i^{(c\bar{c})}$  phase space factor, but do include a  $j_0(kr/2)$  recoil factor. We quote NR results both with and without this recoil factor. The photon energies  $E_\gamma$  depend on the model in most cases, since we have assumed theoretical masses for unknown states.

As with the E1 rates, we quote M1 radiative widths in both the NR potential model of Sec.IIA and the GI model [50] of Sec.IIB. Although the M1 decay rates involve a relatively simple off-diagonal matrix element of the magnetic moment operator, we note that our predicted rates show considerable variation with the model assumptions, and agreement with the two known M1 rates is not good. In the off-diagonal ( $2S \rightarrow 1S$ ) transition  $\psi' \rightarrow \gamma\eta_c$  this is because the zeroth-order M1 matrix element vanishes

due to orthogonality of the spatial wavefunctions, and the nonzero predicted rate results from rather model-dependent corrections to the wavefunctions and recoil effects. Evidently the corrections we have included do not accurately predict the observed partial width; for this reason the other predicted M1 rates between different spatial multiplets are suspect, and in any case are evidently strongly dependent on recoil factors. Better experimental data will be very important for improving our description of these apparently simple but evidently poorly understood M1 radiative transitions.

## IV. OPEN-FLAVOR STRONG DECAYS

### A. The Decay Model

The dominant strong decays (when allowed by phase space) are transitions to open-flavor final states. In these open-flavor decays the initial  $c\bar{c}$  meson decays through production of a light  $q\bar{q}$  quark-antiquark pair ( $q = u, d, s$ ), followed by separation into two open-charm mesons. Remarkably, the QCD mechanism underlying this dominant decay process is still poorly understood. In quark model calculations this decay process is modelled by a simple phenomenological  $q\bar{q}$  pair production amplitude. The  $q\bar{q}$  pair is usually assumed to be produced with vacuum ( $0^{++}$ ) quantum numbers, and variants of the decay model make different assumptions regarding the spatial dependence of the pair production amplitude relative to the initial  $c\bar{c}$  pair. The simplest of these models is the  ${}^3P_0$  model, originally introduced by Micu [54], which assumes that the new  $q\bar{q}$  pair is produced with vacuum quantum numbers ( ${}^3P_0$ ) by a spatially constant pair-production amplitude  $\gamma$ .

LeYaouanc *et al.* subsequently applied the  ${}^3P_0$  model to meson [55] and baryon [56, 57] open flavor strong decays in a series of publications in the 1970s. They also evaluated strong decay partial widths of the three  $c\bar{c}$  states  $\psi(3770)$ ,  $\psi(4040)$  and  $\psi(4415)$  in the  ${}^3P_0$  model [58, 59]; the relation between this early work and our contribution will be discussed.

This decay model, which has since been applied extensively to the decays of light mesons and baryons, was originally adopted largely because of the success in predicting the D/S amplitude ratio in the decay  $b_1 \rightarrow \omega\pi$  [55, 60, 61, 62]. Another stringent test of strong decay models is provided by the very tight limit on the spin singlet to spin singlets transition  $\pi_2(1670) \rightarrow b_1\pi$  from the VES Collaboration [63, 64],

$$B_{\pi_2(1670) \rightarrow b_1\pi} < 1.9 \cdot 10^{-3}, \quad 97.7\% \text{ c.l.} \quad (9)$$

This branching fraction is predicted to be zero in the  ${}^3P_0$  model, but would not necessarily be negligible in a different decay model or if final state interactions are important. (Final state interactions combined with the  ${}^3P_0$  model allow two-stage transitions such as  $\pi_2 \rightarrow \rho\pi \rightarrow b_1\pi$ , although the direct decay  $\pi_2 \rightarrow b_1\pi$  is forbidden in the  ${}^3P_0$  model.)

Recent variants of the  ${}^3P_0$  model modify the pair production vertex [65] or modulate the spatial dependence of the pair production amplitude to simulate a gluonic flux tube [60]. (The latter is the “flux-tube decay model”, which gives very similar predictions to the  ${}^3P_0$  model in practice.)

Another class of decay models assumes that the pair production amplitude transforms as the time component of a Lorentz vector. The Cornell group used a decay model of this type for charmonium [35]. This model appears to describe the partial and total widths of some charmonium states reasonably well, although it is known

to disagree with experimental amplitude ratios in the light quark sector [61].

In this work we employ a formalism that is equivalent to the original constant-amplitude version of the  ${}^3P_0$  decay model, although we have simplified the calculations by deriving momentum-space Feynman rules [61] instead of using the real-space convolution integrals of LeYaouanc *et al.* [55].

In our formalism the  ${}^3P_0$  model describes decay matrix elements using a  $q\bar{q}$  pair production Hamiltonian which is the nonrelativistic limit of

$$H_{decay} = \gamma \sum_q 2m_q \int d^3x \bar{\psi}_q \psi_q. \quad (10)$$

Here  $\psi_q$  is a Dirac quark field,  $m_q$  is the constituent quark mass, and  $\gamma$  is the dimensionless  $q\bar{q}$  pair production amplitude, which is fitted to data. The decay arises from the matrix element of this model Hamiltonian between an initial meson state  $|A\rangle$  and a final meson pair  $|BC\rangle$ , which is nonzero due to the  $b^\dagger d^\dagger$  term. Here we will use SHO (simple harmonic oscillator) wavefunctions for the mesons, with a universal width parameter  $\beta$ . The pair-production strength parameter  $\gamma$  is found to be roughly flavor-independent in light meson decays involving pair production of  $u\bar{u}$ ,  $d\bar{d}$  and  $s\bar{s}$  pairs. In our recent extensive studies of light ( $u, d, s$ ) meson decays [61, 66, 67] we found that the value

$$\gamma = 0.4 \quad (11)$$

gives a reasonably accurate description of the overall scale of decay widths.

### B. Charmonium Strong Decays

#### 1. Previous studies

The open-flavor decay amplitudes of the three  $c\bar{c}$  states  $\psi(3770)$ ,  $\psi(4040)$  and  $\psi(4415)$  were evaluated in the  ${}^3P_0$  model by LeYaouanc *et al.* in the late 1970s [58, 59]. Their calculations are generally quite similar to the approach used here, although we note three important differences:

- 1) LeYaouanc *et al.* fitted the pair production strength  $\gamma$  and wavefunction length scale  $R$  to the charmonium decay data, whereas we used the same pair production amplitude  $\gamma$  as in light meson decays, and our SHO wavefunction length scale  $\beta^{-1}$  is taken from  $c\bar{c}$  potential models.
- 2) We use the correct reduced mass coordinates for the unsymmetric open-charm meson wavefunctions, whereas LeYaouanc *et al.* assumed symmetric SHO wavefunctions for all mesons. This approximation proves to be quite important numerically, since  $m_c \gg m_s, m_{u,d}$ .
- 3) We consider all energetically allowed open-flavor decay modes. LeYaouanc *et al.* did not consider some S+P

decays of the  $\psi(4415)$ , nor did they consider the important  $J^P = 1^+$  D meson singlet-triplet mixing angle. (The masses of the P-wave charmed mesons were unknown at that time.)

Although we have improved on the earlier calculations of LeYaouanc *et al.*, and evaluate a much more extensive set of decay amplitudes, we do concur with their important conclusion that the DD mode of the  $\psi(4040)$  is naturally suppressed given a  $3^3S_1$   $c\bar{c}$  assignment, and also that S+P modes are important for the  $\psi(4415)$ .

Other more recent applications of the  $^3P_0$  decay model to charmonium include a study of the strong decays of various  $c\bar{c}$  X(3872) candidates to DD [26], and an examination of the hypothesis that the  $\psi(4040)$  and  $\psi(4160)$  are linear superpositions of a  $c\bar{c}$  hybrid and a conventional  $\psi(3S)$   $c\bar{c}$  state [68].

The only other detailed studies of the open-flavor strong decays of charmonia of which we are aware are the early work by the Cornell group [35], and recent more detailed applications of this model to other charmonium states [27]. The decay model of the Cornell group assumes a pair creation operator which is the time component of a Lorentz vector ( $j^0$ ), rather than the Lorentz scalar assumed by the  $^3P_0$  model. As we noted previously, this  $j^0$  model does not agree well with some light meson decay amplitude ratios. In the original Cornell model decay calculations only the combined channel contributions to  $R$  were derived, and only channels containing pairs of S-wave open-charm mesons were included. The very interesting relative amplitudes in the  $D^*D^*$  channel have not been evaluated in this model.

## 2. This study

Tables X-XV present the partial widths and strong decay amplitudes we find for all kinematically allowed open-flavor decay modes of all the charmonium states listed in Table I. We have evaluated these in the  $^3P_0$  model, assuming SHO wavefunctions with a width parameter of  $\beta = 0.5$  GeV and a pair production amplitude of  $\gamma = 0.4$ . SHO wavefunctions have the advantage that the decay amplitudes can be determined analytically, and we have found that the numerical results are usually not strongly dependent on the details of the spatial wavefunctions [60, 61, 69, 70], unless they are near a node. This width parameter was chosen by comparing the overlap of NR and GI potential model wavefunctions with SHO wavefunctions, which was found to be largest for both charmonium and open-charm mesons for a  $\beta$  near 0.5 GeV.

As a test of the accuracy of these parameters, especially the value assumed for the  $q\bar{q}$  pair production amplitude  $\gamma$  (which is taken from light meson decays), in Fig. 2 we compare the predicted total widths for  $\beta = 0.5$  GeV and variable  $\gamma$  to the values observed for the four known  $c\bar{c}$  states above open-charm threshold,  $\psi(3770)$ ,  $\psi(4040)$ ,  $\psi(4159)$  and  $\psi(4415)$ . Although there is some scatter

in the value of  $\gamma$  specified by these widths, a choice of  $\gamma = 0.35$  is evidently near optimum, and yields an average error of only 29%, which is very reasonable for this phenomenological model. In the decay tables we will quote numerical results for our standard light-meson value of  $\gamma = 0.4$ , which is rather close to this value. A subsequent change in  $\gamma$  will simply scale the widths as  $\gamma^2$ .

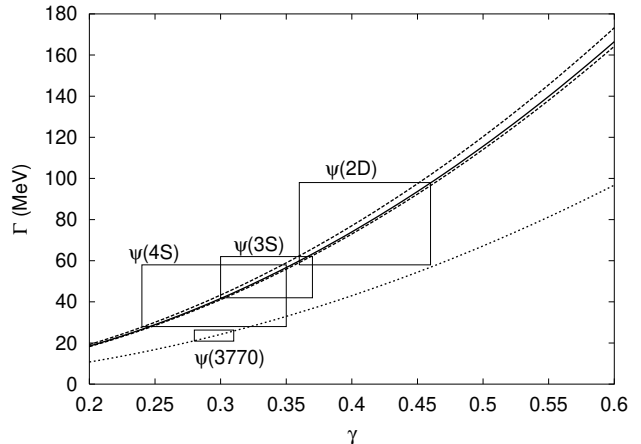


FIG. 2: Values of the  $^3P_0$  decay model pair production strength  $\gamma$  implied by the experimental total widths of the known higher-mass vector states  $\psi(3770)$ ,  $\psi(4040)$ ,  $\psi(4159)$  and  $\psi(4415)$ . This calculation assumes pure  $c\bar{c}$  spectroscopic states, respectively  $1^3D_1$ ,  $3^3S_1$ ,  $2^3D_1$  and  $4^3S_1$ . The boxes show current PDG experimental width uncertainties.

For this paper the strong decay amplitudes were first evaluated analytically, following which numerical values were determined given our parameters  $\beta = 0.5$  GeV,  $\gamma = 0.4$ , and our constituent quark masses  $m_{u,d} = 0.33$  GeV,  $m_s = 0.55$  GeV and  $m_c = 1.5$  GeV. (Quark mass ratios are required to specify the final open-charm meson wavefunctions.) We determine the decay kinematics using external meson masses taken from the Particle Data Group [64] (charge averaged where appropriate) and from recent Belle results [71]. These masses are  $M_D = 1.867$  GeV,  $M_{D^*} = 2.008$  GeV,  $M_{D_0^*} = 2.308$  GeV [71],  $M_{D_1(\text{narrow})} = 2.425$  GeV,  $M_{D_1'(\text{broad})} = 2.427$  GeV [71],  $M_{D_2^*} = 2.459$  GeV,  $M_{D_s} = 1.968$  GeV,  $M_{D_s^*} = 2.112$  GeV,  $M_{D_{s0}^*} = 2.317$  GeV,  $M_{D_{s1}} = 2.459$  GeV. The FOCUS collaboration [72] estimate a somewhat higher mass for the scalar  $D_0^*$ , however their result is complicated by the presence of both scalar and broad axial vector ( $D_1'$ ) contributions [73].

The  $J^P = 1^+$  axial vector  $c\bar{n}$  and  $c\bar{s}$  mesons  $D_1$  and  $D_1'$  are assumed to be coherent superpositions of quark model spin-singlet and spin-triplet states,

$$\begin{aligned} |D_1\rangle &= +\cos(\theta)|^1P_1\rangle + \sin(\theta)|^3P_1\rangle \\ |D_1'\rangle &= -\sin(\theta)|^1P_1\rangle + \cos(\theta)|^3P_1\rangle. \end{aligned} \quad (12)$$

We define this singlet-triplet mixing angle in the LS coupling scheme, in accord with the conventions of Ref.[67].

This reference also discusses other conventions for this mixing angle that have appeared in the literature. In the heavy-quark limit we expect to find a “magic” mixing angle, due to the quark mass dependence of the spin-orbit and tensor terms, which is  $\theta = 35.3^\circ (-54.7^\circ)$  if the expectation of the heavy-quark spin-orbit interaction is negative (positive) [74]. In the following we assume the first case, which is supported by the reported widths of the  $1^+ P$ -wave  $c\bar{c}n$  mesons. We note however that finite quark mass effects and mixing induced by higher-order Fock states can substantially modify this mixing angle, so it should more generally be treated as a free parameter. We will discuss the dependence of our strong decay amplitudes on this mixing angle for a few sensitive cases.

## V. DISCUSSION OF $c\bar{c}$ STATES

### A. Known states above 3.73 GeV

The four known  $c\bar{c}$  states above DD threshold,  $\psi(3770)$ ,  $\psi(4040)$ ,  $\psi(4159)$  and  $\psi(4415)$  are of special interest because they are easily produced at  $e^+e^-$  machines. Accordingly we will first discuss our predicted strong decay amplitudes and widths for these states. This will be followed by a more general discussion of  $c\bar{c}$  strong decays by multiplet.

#### 1. $\psi(3770)$

The  $\psi(3770)$  is generally assumed to be the  $^3D_1$   $c\bar{c}$  state, perhaps with a significant  $2^3S_1$  component [75, 76]. (This additional component can explain the leptonic width, which is much larger than expected for a pure  $^3D_1$   $c\bar{c}$  state [45].)

For a pure  $^3D_1$  state at the  $\psi(3770)$  mass we predict a DD width of 43 MeV with our parameters, which is rather larger than the experimental value of  $23.6 \pm 2.7$  MeV. The partial width of a mixed 2S-D state

$$|\psi(3770)\rangle = +\cos(\theta)|^3D_1\rangle + \sin(\theta)|2^3S_1\rangle \quad (13)$$

is shown in Fig. 3 as a function of the mixing angle  $\theta$ . In this simple model, fitting the experimental  $\psi(3770)$  width requires a mixing angle of  $\theta = -17.4^\circ \pm 2.5^\circ$ . Assuming that the leptonic widths scale as the S-wave component squared, this mixing angle predicts an  $e^+e^-$  partial width ratio of

$$\left. \frac{\Gamma_{e^+e^-}(\psi(3770))}{\Gamma_{e^+e^-}(\psi(3686))} \right|_{thy.} = 0.10 \pm 0.03 . \quad (14)$$

It is interesting that this is consistent with experiment,

$$\left. \frac{\Gamma_{e^+e^-}(\psi(3770))}{\Gamma_{e^+e^-}(\psi(3686))} \right|_{expt.} = 0.12 \pm 0.02 , \quad (15)$$

so the small  $\psi(3770)$  total width may indeed be an effect of  $^3D_1 - 2^3S_1$  mixing.

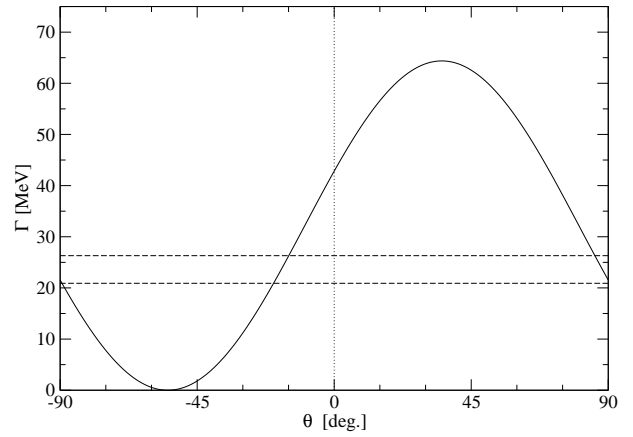


FIG. 3: The total width of the  $\psi(3770)$  as a function of the  $^3D_1 - 2^3S_1$  mixing angle  $\theta$ . The experimental  $1\sigma$  limits are shown as horizontal dashed lines.

#### 2. $\psi(4040)$

Next in mass is the  $\psi(4040)$ , which is a very interesting case for the study of strong decays. Four open-charm modes are energetically allowed, DD,  $DD^*$ ,  $D^*D^*$  and  $D_sD_s$ , although  $D^*D^*$  has little phase space. There is some experimental evidence for the three nonstrange modes from Mark I at SLAC [77]. Remarkably, the reported relative branching fractions (scaled by  $p^3$ ) show a very strong preference for  $D^*$  final states,  $D^{*0}D^{*0} \gg D^0D^{*0} \gg D^0D^0$ . This motivated suggestions that the  $\psi(4040)$  might be a  $D^*D^*$  molecule [78, 79, 80]. The Mark I results were

$$\begin{aligned} \frac{B}{p^3}(D^{*0}D^{*0} : D^0D^{*0} : D^0D^0) = \\ 128 \pm 40 : 4.0 \pm 0.8 : 0.2 \pm 0.1 . \end{aligned} \quad (16)$$

This is much less striking once the  $p^3$  factors are restored, which gives

$$B(D^{*0}D^{*0} : D^0D^{*0} : D^0D^0) = \\ 1 \pm 0.31 : 0.95 \pm 0.19 : 0.12 \pm 0.06 , \quad (17)$$

where we have used the  $D^{*0}D^{*0}$  mode to set the scale. These relative branching fractions should be compared to our theoretical  $\psi(4040)$  branching fractions, not the more often quoted  $B/p^3$  ratios.

Comparison with Table X shows that the predicted  $^3P_0$  model partial and total widths for a  $3^3S_1$   $\psi(4040)$  state are actually in accord with the Mark I results. The total width is predicted to be 74 MeV, which is reasonably close to the PDG experimental average of  $52 \pm 10$  MeV. Seth [81] estimates a rather larger width of  $88 \pm 5$  MeV for this state from Crystal Ball and new BES data, which is closer to our predicted width.

The  $DD^*$  and  $D^*D^*$  branching fractions are predicted to be approximately equal, consistent with Mark I.

The DD mode is predicted to be much smaller, despite its larger phase space, as it is accidentally near a node in the  $^3P_0$  model decay amplitude. (This was previously noted by LeYaouanc *et al.* [58].) This set of predictions constitutes a very nontrivial success of the  $^3P_0$  decay model. The actual width to the suppressed DD mode is probably a few MeV; the 0.1 MeV quoted in the table depends strongly on the location of the node, and varying the SHO width parameter  $\beta$  by  $\pm 10\%$  suggests that a DD partial width of a few MeV is plausible. This is again consistent with the Mark I result.

The  $D^*D^*$  mode is especially interesting for strong decay studies, since there are three independent decay amplitudes for  $1^{--} c\bar{c} \rightarrow D^*D^*$ ,  $^1P_1$ ,  $^5P_1$  and  $^5F_1$ . If the  $\psi(4040)$  is a pure S-wave  $c\bar{c}$  state, we predict a zero  $^5F_1 D^*D^*$  decay amplitude, and the ratio of the nonzero amplitudes is  $^5P_1/{}^1P_1 = -2\sqrt{5}$  (independent of the radial wavefunction). As we shall see when we discuss the  $\psi(4159)$ , very different  $D^*D^*$  amplitude ratios are predicted for a  $^3D_1$  initial  $c\bar{c}$  state.

The unobserved mode  $D_sD_s$  is predicted to have a branching fraction of about 11%; this prediction is fortunately not especially sensitive to the location of the decay amplitude node for  $\psi(4040)$  to two pseudoscalars. This branching fraction is of special interest because it determines the event rates available for studies of  $D_s$  weak decays at  $e^+e^-$  colliders such as CLEO.

Finally, we note that a large sample of  $\psi(4040)$  events might be used to access the  $2P c\bar{c}$  multiplet, since the E1 radiative branching fractions for  $\psi(4040) \rightarrow \gamma\chi'_J$  are expected to be *ca.*  $10^{-3}$  (Table II).

### 3. $\psi(4159)$

Comparison of the mass of the  $1^{--} \psi(4159)$  with potential model predictions (Fig. 1) immediately suggests a  $2^3D_1 c\bar{c}$  assignment. There may also be a significant S-wave  $c\bar{c}$  component, since the  $\psi(4159)$  has a much larger  $e^+e^-$  width than one would expect for a pure D-wave  $c\bar{c}$  state [45]. (This was also the case for the  $\psi(3770)$ .)

There are five open-flavor decay modes available to a  $1^{--} c\bar{c}$  vector at this mass, DD,  $DD^*$ ,  $D^*D^*$ ,  $D_sD_s$  and  $D_sD_s^*$ . The predicted decay amplitudes and partial widths for a  $2^3D_1 \psi(4159)$  are given in Table XII. The theoretical total width of 74 MeV is in good agreement with the experimental value of  $78 \pm 20$  MeV. Seth [81] quotes a similar width of  $107 \pm 8$  MeV for this state from Crystal Ball and recent BES data.

The leading mode is predicted to be  $D^*D^*$  with a branching fraction of  $\approx 50\%$ , followed by comparable DD and  $D_sD_s^*$  modes (both  $\approx 20\%$ ), and a somewhat weaker  $D_sD_s$  ( $\approx 10\%$ ). The  $DD^*$  branching fraction is predicted to be very small, since it is suppressed by a decay amplitude node near the physical point.

The mode  $D^*D^*$  is again especially interesting, due to the three decay amplitudes allowed for this final state. (The other modes have only single amplitudes.) For a

pure D-wave  $c\bar{c}$  assignment the ratio of the two  $D^*D^*$  P-wave amplitudes is independent of the radial wavefunction, and is  $^5P_1/{}^1P_1 = -1/\sqrt{5}$ . The  $^5F_1$  amplitude is predicted to be the largest given this  $2^3D_1$  assignment, whereas it is zero for an S-wave  $c\bar{c}$  state. Clearly, a determination of these  $D^*D^*$  decay amplitude ratios would be an extremely interesting test of decay models. Experimentally, to date nothing has been reported regarding the exclusive hadronic decay modes of the  $\psi(4159)$ .

### 4. $\psi(4415)$

The final  $c\bar{c}$  resonance known above DD threshold is the  $1^{--} \psi(4415)$ . Again, the mass of this resonance relative to potential model predictions suggests a  $c\bar{c}$  assignment, in this case  $4^3S_1$ . Of course this identification requires independent confirmation, since  $c\bar{c}$  hybrids are predicted to first appear near this mass by LGT simulations [37, 38, 39, 40], and the lightest hybrid multiplet in the flux tube model includes a  $1^{--}$  state [82].

Ten open-charm strong decay modes are allowed for the  $\psi(4415)$ , seven with  $c\bar{n}$  meson final states ( $n = u, d$ ), and three with  $c\bar{s}$ . The predicted branching fractions of a  $4^3S_1 c\bar{c}$  state at this mass are quite characteristic, and (if the  $^3P_0$  decay model is accurate) may be useful in confirming this assignment. As a note of caution, a  $4S$  state has three radial nodes, and some of the smaller predicted branching fractions are sensitive to the locations of the nodes.

The predicted total width of a  $4^3S_1 c\bar{c}$  meson at this mass with our parameters is 77 MeV, somewhat larger than the experimental PDG average width of  $43 \pm 15$  MeV. Seth [81] notes however that the width of this state in Crystal Ball and recent BES data is rather larger, and quotes an average of  $119 \pm 15$  MeV, on the opposite side of the  $^3P_0$  decay model prediction.

The largest exclusive mode is predicted to be the S+P combination  $DD_1$ , where  $D_1$  is the narrower of the two  $1^+ c\bar{n}$  axial mesons near 2.42-2.43 GeV. Since the  $D_1$  is rather narrow ( $\Gamma \approx 20$ -30 MeV) and decays dominantly to  $D^*\pi$ , there should be a strong  $\psi(4415)$  signal in  $DD^*\pi$  final states. Although both S-wave and D-wave  $DD_1$  final states are allowed, in the  $^3P_0$  model the HQET (heavy quark effective theory)  $D_1$  mixing angle  $\theta$  is just the value needed to give a zero S-wave  $\psi(4415) \rightarrow DD_1$  amplitude. Thus we have the striking prediction that the dominant  $\psi(4415)$  decay mode is  $DD_1$ , in D-wave rather than S-wave.

The second-largest  $\psi(4415)$  branching fraction is predicted to be another S+P mode,  $DD_2^*$ . The  $D_2^*$  is also moderately narrow, so this isobar can also be isolated from the observed final state. (The PDG quotes a neutral  $D_2^*$  total width of  $\Gamma = 23 \pm 5$  MeV, but Belle [71] and FOCUS [83] find somewhat broader values of  $\Gamma = 45.6 \pm 8.0$  MeV and  $\Gamma = 38.7 \pm 5.3 \pm 2.9$  MeV respectively; see [84] for a recent discussion. The  $D_2^*$  has significant branching fractions to both  $D^*\pi$  and  $D\pi$ , so



the  $DD_2^*$  mode of the  $\psi(4415)$  should be observable in both  $DD\pi$  and  $DD^*\pi$ .

A final important  $\psi(4415)$  mode is predicted to be  $D^*D^*$ , which should be comparable in strength to  $DD_2^*$ . As noted in the previous discussions of  $\psi(4040)$  and  $\psi(4159)$  decays,  $D^*D^*$  is an especially interesting decay mode because it has three amplitudes, and the  ${}^5P_1/{}^1P_1$  amplitude ratio is independent of the radial wavefunction for pure S-wave or D-wave  $c\bar{c}$  states. If the  $\psi(4415)$  is indeed an S-wave ( $4^3S_1$ )  $c\bar{c}$  state to a good approximation, we expect this ratio to be  ${}^5P_1/{}^1P_1 = -2\sqrt{5}$ , and the  ${}^5F_1$  amplitude should be zero.

It is interesting to note that  $\psi(4415)$  decays may provide access to the recently discovered  $D_{s0}^*(2317)$ . Although the channel  $D_s^*D_{s0}^*(2317)$  has a threshold of 4429 MeV, 14 MeV above the nominal mass of the  $\psi(4415)$ , the width of the  $\psi(4415)$  and the fact that the decay  $\psi(4415) \rightarrow D_s^*D_{s0}^*(2317)$  is purely S-wave implies that one may observe significant  $D_{s0}^*(2317)$  production just above threshold, near  $E_{cm} \approx 4435$  MeV. This is illustrated in Fig. 4, in which we show theoretical  ${}^3P_0$  decay model partial widths to  $D_s^*D_{s0}^*(2317)$  and  $D_sD_{s1}(2459)$  as functions of the  $4^3S_1$   $c\bar{c}$  mass. (This calculation assumes pure  $c\bar{c}$   $D_{s0}^*(2317)$  and  $D_{s1}(2459)$  states, and should be modified accordingly if they have significant non- $c\bar{c}$  components.) Unfortunately,  $\psi(4415)$  decays are not expected to be similarly effective in producing the  $D_{s1}(2459)$ , because the assumed “magic-mixed” HQET state  $|D_{s1}(2459)\rangle = \sqrt{1/3} |{}^3P_1(c\bar{s})\rangle + \sqrt{2/3} |{}^1P_1(c\bar{s})\rangle$  predicts a vanishing  $\psi(4415) \rightarrow D_sD_{s1}$  S-wave decay amplitude.

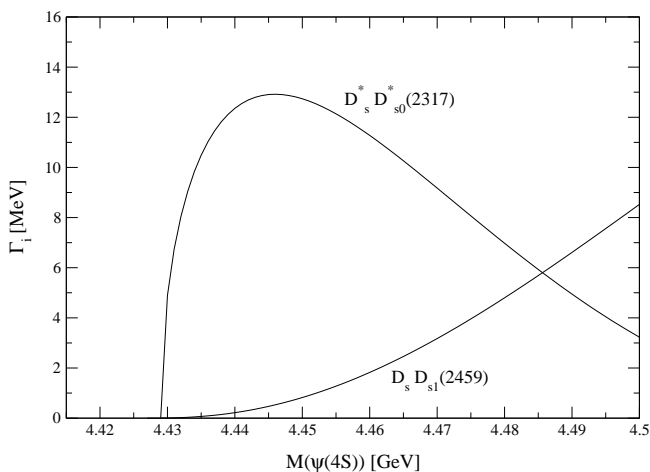


FIG. 4: Partial widths predicted for  $\psi(4^3S_1) \rightarrow D_s^*D_{s0}^*(2317)$  and  $D_sD_{s1}(2459)$  as a function of the assumed  $\psi(4^3S_1)$  mass.

## B. 3S and 4S states

The two unknown states in the 3S and 4S multiplets are the  $3^1S_0$  and  $4^1S_0$  pseudoscalars. To evaluate their strong decays we have assigned potential model masses to these states, specifically 4043 MeV and 4384 MeV. The resulting total widths are predicted to be moderate, 80 MeV and 61 MeV respectively, and both states should be observable in  $DD^*$  and  $D^*D^*$  (see Table X). No other open-charm strong decay modes are allowed for a  $3^1S_0$   $\eta_c(4043)$ . Although these modes are also important for the  $4^1S_0$   $\eta_c(4384)$ , its largest branching fraction is predicted to be to the S+P combination  $DD_2^*$  ( $\approx 40\%$ ).

These states may be observable in  $\gamma\gamma$  and hadronic production (through  $gg$  fusion), analogous to the  $\eta_c$  and  $\eta_c'$ . M1 transitions from the higher vectors to these states are unfortunately predicted to be rather weak, since they are either hindered or have little phase space. (See Table IX.)

## C. 2P states

The mean 2P multiplet mass is predicted to be near 3.95 GeV. There is an interesting disagreement between the NR and GI models regarding the scale of mass splittings within this multiplet, as well as in the 3P states. (See Table I and Fig. 1.)

There are few open-flavor strong modes available to the 2P states (Table XI). One result of this restricted phase space is the prediction of a fairly narrow  $2^3P_0$   $\chi_0(3852)$  (assuming the NR model mass) that decays only to  $DD$ , with a total width of just 30 MeV. This small width is due in part to a decay amplitude node, and a variation of the total width by a factor of two could easily be accommodated. The two axial states  $2^3P_1$   $\chi_1(3925)$  and  $2^1P_1$   $h_c(3934)$  can only decay to  $DD^*$ , and both have nonzero S- and D-wave decay amplitudes; their D/S ratios are  $-0.18$  and  $+0.46$  respectively. Observation of the D/S ratio in a  $DD^*$  enhancement could be a useful check of the assumption of a resonant  $1^+ c\bar{c}$  contribution.

The relatively narrow  $2^3P_0$  state  $\chi_0(3852)$  can be produced in  $\gamma\gamma$ , as can its somewhat wider  $2^3P_2$   $\chi_2(3972)$  partner. Additional possible production mechanisms include  $gg$  fusion (for the  $2^3P_0$  and  $2^3P_2$ ), E1 radiative transitions from higher  $1^{--} c\bar{c}$  states (to all 2P  $\chi_J$  states), and B decays. The E1 branching fractions of the  $\psi(4040)$  and  $\psi(4159)$  to 2P  $\chi_J$  states are predicted to be sufficiently large (*ca.*  $10^{-3}$ , see Tables II,V) to allow identification of these states at BES and CLEO.

Although no 2P  $c\bar{c}$  state has been clearly established experimentally, there are two recent reports of enhancements which may be due to states in this multiplet. The Belle Collaboration has reported evidence of an enhancement in  $\omega J/\psi$  with a mass and width of  $3941 \pm 11$  MeV and  $92 \pm 24$  MeV [85]; this is compatible with expectations for 2P  $\chi_J c\bar{c}$  states. (Although 2P  $c\bar{c}$  states should strongly favor open-charm strong decay modes,

inelastic FSIs (final state interactions) will allow weaker transitions to closed-charm final states such as  $\omega J/\psi$ . These FSIs should be most important in S-wave, as in the virtual second-order processes  $\chi_{0,2}(3940) \rightarrow D^*D^* \rightarrow \omega J/\psi$ . A search for evidence of this state in open-charm final states, with much larger branching fractions than to  $\omega J/\psi$ , will be a crucial test of a charmonium assignment. Assuming that the enhancement is indeed due to a 2P  $\chi_J$  state, if it is the  $0^{++}$  state it will populate only DD, if  $1^{++}$  only  $DD^*$ , and if  $2^{++}$  comparable branching fractions to DD and  $DD^*$  are expected.

There is a second report of a possible 2P state, also from the Belle Collaboration [33], in double charmonium production. An enhancement is seen in  $e^+e^- \rightarrow J/\psi DD^*$  at a mass of  $3940 \pm 12$  MeV, with a limit on the total width of  $< 96$  MeV (90% *c.l.*). As this enhancement is not seen in  $\omega J/\psi$ , it has been suggested [34] that it is distinct from the 3940 MeV signal discussed above. Consideration of possible 2P candidates (Table XI) suggests that this enhancement may be due to the  $\chi_{c1}(2P)$ , which is predicted to have a similar mass of 3925 MeV. (The predicted total width however is a somewhat larger 165 MeV.)

#### D. 3P states

The 3P states have an expected mean multiplet mass of about 4.3 GeV. As with the 2P states there is a significant difference between the NR and GI models in the scale of mass splittings predicted within the multiplet. This leads for example to a 90 MeV difference between the models for the predicted mass of the  $3^3P_0$  scalar.

Many open-charm strong decay channels are open at the 3P mass scale. The individual decay amplitudes however are typically somewhat smaller than for the 2P states, due in part to nodes in the decay amplitudes. This has the interesting result that the predicted mean total width of 3P states is smaller than for 2P states (58 MeV for 3P versus 91 MeV for 2P).

The predicted branching fraction to the mode  $D^*D^*$  is large for all four 3P states, and is the largest for all except the spin-singlet  $3^1P_1$   $h_c(4279)$ ; in this case the leading mode is  $DD_0^*$ . For all 3P states except the  $3^3P_1$  the  $D^*D^*$  decay mode has multiple amplitudes, which are predicted to be comparable in strength. An experimental determination of any of these amplitude ratios would provide an interesting test of decay models. The decays of the tensor  $3^3P_2$   $\chi_2(4317)$  to  $DD_1$  and  $DD_1'$  are also interesting, in that the prediction that the broad  $D_1'$  mode dominates is a test of the axial-D mixing angle.

As with the 2P states, the most important experimental problem is to find an effective production mechanism. Again,  $\gamma\gamma$  and  $gg$  fusion can produce the  $2^{++}$  and  $0^{++}$  states (here  $3^3P_2$  and  $3^3P_0$ ), although there should be moderate suppression of the production amplitudes relative to the 1P ground states due to the higher masses and smaller short-distance  $c\bar{c}$  wavefunctions. E1 transitions

from the  $\psi(4415)$  could lead to the identification of the 3P states, since radiative partial widths of 50-100 keV are expected to the  $3^3P_2$  and  $3^3P_1$ ; these correspond to branching fractions of *ca.*  $10^{-3}$ . Production of the  $3^3P_0$  state however is expected to be suppressed, due to a radiative decay amplitude node.

#### E. 1D states

Since the  $3^3D_2$  and  $1^1D_2$  states do not have allowed open-flavor decay modes, and we have already considered  $3^3D_1$  decays in the section on the  $\psi(3770)$ , we restrict our discussion to the  $3^3D_3$ . This currently unknown state is predicted to have a mass of 3806 MeV in the NR potential model. It is expected to be quite narrow simply because it has little phase space to the only open-flavor mode DD, which has an F-wave centrifugal barrier; with our parameters the predicted total strong width is just 0.5 MeV. The radiative width for the E1 transition  $\psi_3(3806) \rightarrow \gamma\chi_2$  is predicted to be about 0.3 MeV (Table V), so the total width of this  $3^3D_3$  state should be near 1 MeV, with comparable strong and radiative branching fractions.

Finding an effective production mechanism for this interesting state is again a crucial problem. As it has  $C = (-)$ , it cannot be made in  $\gamma\gamma$  or  $gg$  fusion. One possibility is that the  $3^3D_3$  may be observable in E1 transitions from the radial  $2^3P_2$  tensor, since the radiative partial width is predicted to be a relatively large  $\approx 100$  keV. Similarly, the narrow  $3^3D_2$  and  $1^1D_2$  states may be observable in E1 transitions from 2P states, assuming that a production mechanism can be found for 2P states. All three of these states can also be produced in B-decays [14].

#### F. 2D states

The states in the 2D multiplet are predicted to be essentially degenerate in both the NR and GI potential models. The  $2^3D_1$  candidate  $\psi(4159)$  suggests a 2D multiplet mass near 4.16 GeV, which is consistent with potential model expectations. Since the  $\psi(4159)$  was discussed previously, here we will consider only the unknown states  $2^3D_3$ ,  $2^3D_2$  and  $2^1D_2$ .

These states are predicted to be rather broad, with theoretical total widths ranging from 78 MeV for the  $2^3D_1$  (consistent with the  $\psi(4159)$ ) to 148 MeV for the  $2^3D_3$ . The energetically allowed open-flavor modes are all of S+S type, since the first S+P mode is  $DD_0^*$ , at a nominal mass of 4175 MeV. The decays of 2D states are dominated by DD,  $DD^*$  and  $D^*D^*$ , with smaller contributions from the charm-strange final states  $D_sD_s$  and  $D_sD_s^*$ .

If these states (besides the  $\psi(4159)$ ) can be produced, there are several interesting tests of their strong decay amplitudes. The  $2^3D_3$   $\psi_3(4167)$ , for example, is predicted to have  $D^*D^*$  as the dominant mode, with both

$^1F_3$  and  $^5F_3$  amplitudes present, in the ratio  $^5F_3/^1F_3 = -\sqrt{24/5}$ . The remaining 2D states have many multi-amplitude decays, in which the higher-L partial waves have large or dominant amplitudes. (Compare the P- and F-waves in the decays in Table XII.)

### G. 1F states

The four states in the 1F multiplet are predicted to be almost degenerate in both the NR and GI models, although the models disagree somewhat regarding this mass. In the NR potential model the states are expected near 4025 MeV, whereas in the GI model the expected mass is near 4095 MeV. This discrepancy is mainly due to the different values assumed for the string tension.

It is unfortunate that production amplitudes for these higher-L states are expected to be quite weak, since the 1F multiplet is predicted to contain a rather narrow state, the  $^3F_4 \chi_4$  (Table XIII). Assuming our NR model  $^3F_4$  mass of 4021 MeV, we predict a strong width for this state of just 8.3 MeV. This is partly a result of the centrifugal barrier (both open modes, DD and DD\*, are G-waves), and is also because there is essentially no phase space for D\*D\*. If the GI masses are more accurate we would no longer expect a very narrow  $^3F_4$  state, since the D\*D\* partial width increases rapidly above threshold. At the GI mass of 4095 MeV the  $^3F_4$  is predicted to have a partial width to D\*D\* of 38 MeV, and a total width of 60 MeV.

The single well-established mechanism that might be exploited to produce a 1F state is an E1 radiative transition from the  $\psi(4159)$  to the  $^3F_2 \chi_2$ . This transition however has a rather weak, model-dependent partial width of 20-50 keV (Table V), and the  $^3F_2$  is predicted to be the broadest 1F state, with a total width of about 160 MeV.

If an effective production mechanism for 1F states is identified, the E1 decays of these states can be used to populate the narrow 1D states; the E1 transitions  $^3F_4 \rightarrow ^3D_3$ ,  $^3F_3 \rightarrow ^3D_2$  and  $^1F_3 \rightarrow ^1D_2$  are predicted to have rather large radiative widths of *ca.* 300-400 keV (see Table VI).

### H. 2F and 1G states

To complete our study we have evaluated the spectrum and decays of all states in the 2F and 1G multiplets (Tables XIV and XV), although the lack of a clear experimental route to these states suggests that it may be quite difficult to test these predictions.

The multiplets are again predicted to be nearly degenerate in both the NR and GI potential models, with somewhat lower masses predicted by the NR model. The mean 2F and 1G masses are approximately 4350 MeV and 4225 MeV respectively in the NR model, and 4425 MeV and 4320 MeV in the GI model.

Assuming NR model masses, these states are predicted to have total widths that range from a minimum of 58 MeV for the  $^3G_5 \psi_5(4214)$  to a maximum of 180 MeV for the  $^2^3F_2 \chi_2(4351)$ . The individual decay modes do show some interesting features; although the dominant modes are usually of S+S type, some S+P modes are important in 2F decays. For example, the largest decay modes of the  $^2^3F_3 \chi_3(4352)$  and  $^2^3F_2 \chi_2(4351)$  are both S+P, with branching fractions of  $B(\chi_3 \rightarrow DD_2^*) = 30\%$  and  $B(\chi_2 \rightarrow DD_1) = 59\%$  respectively.

## VI. SUMMARY AND CONCLUSIONS

We have computed the spectrum, all allowed E1 and some M1 electromagnetic partial widths, and all allowed open-charm strong decay amplitudes of the 40 charmonium states expected to *ca.* 4.4 GeV. These were evaluated using two potential models, the quark model formulation of electromagnetic transition amplitudes, and the  $^3P_0$  strong decay model.

The predictions of the spectrum should be useful in the identification of new states, and in tests of the Lorentz structure of confinement and the nature of spin-dependent forces. The transition amplitudes will be useful in searches for new higher-mass  $c\bar{c}$  states, as they suggest which final states should be populated preferentially by the decays of a given initial  $c\bar{c}$  state, as well as predicting the often characteristic strong decay amplitude ratios within a given final state. These predictions may also be useful in distinguishing between conventional charmonia and exotica such as charmed meson molecules (perhaps including the X(3872)) and  $c\bar{c}$  hybrids. These results all implicitly test the accuracy of the pure- $c\bar{c}$  assumption made in these models, and can serve as benchmarks for calculations that relax this assumption.

Future experimental measurements of strong partial widths and decay amplitude ratios can provide very important tests of strong decay models, the  $^3P_0$  model in particular. We have discussed many specific examples of these tests in the previous sections; here we will summarize some of our most important observations.

The  $\psi(3770)$  is the lightest known  $c\bar{c}$  state above open-charm threshold. We noted that the relatively large  $e^+e^-$  width of the  $\psi(3770)$  is difficult to understand if it is assumed to be a pure  $^3D_1 c\bar{c}$  state, but this problem is solved if the  $\psi(3770)$  has a significant admixture of the  $2^3S_1 c\bar{c}$  basis state. This mixing also solves the  $\psi(3770)$  total width problem, since the mixing angle required to fit the  $e^+e^-$  width is consistent with the value required to fit the  $^3P_0$  model DD strong width to experiment. This mixing angle has been discussed in earlier references (see for example Refs.[75, 76]), although the observation that the same mixing angle resolves both the  $e^+e^-$  and total width discrepancies has not been noted previously.

The relative branching fractions of the  $\psi(4040)$  to DD, DD\* and D\*D\*, although often cited as anomalous, are naturally explained in the  $^3P_0$  model by a node in the DD

decay amplitude. A very important test of this strong decay model and the nature of the  $\psi(4040)$  follows from a simple measurement of the ratios of the three independent  $D^*D^*$  decay amplitudes. The  $^3P_0$  model predicts that the  $^5F_1$  amplitude is zero, and the ratio of the two P-wave amplitudes is  $^5P_1/1P_1 = -2\sqrt{5}$ , independent of the radial wavefunction, provided that the  $\psi(4040)$  is a pure S-wave  $c\bar{c}$  state. Similarly, the  $D^*D^*$  amplitude ratios in  $\psi(4159)$  decays test the decay model and the assumed  $2^3D_1$  assignment for this state. The  $^5F_1$   $D^*D^*$  amplitude is predicted to be the largest for a pure  $2^3D_1$   $\psi(4159)$ , and the P-wave amplitude ratio is predicted to be  $^5P_1/1P_1 = -1/\sqrt{5}$ , again independent of the radial wavefunction. Finally, we noted that it may be possible to identify a higher-L  $c\bar{c}$  state (the  $^3F_2$   $\chi_2$  member of the F-wave  $c\bar{c}$  multiplet) in E1 radiative  $\psi(4159)$  decays.

The  $\psi(4415)$  has ten open-flavor modes, and their branching fractions have never been determined. We predict that the largest is the unusual S+P combination  $DD_1$ . It is especially notable that strong decays of the  $\psi(4415)$  may provide a novel production mechanism for the enigmatic  $D_{s0}^*$  (2317), through the above-threshold decay  $\psi(4415 + \epsilon) \rightarrow D_s^* D_{s0}^*$  (2317), as shown in Fig. 4. One may also produce higher-mass charmonium states from the  $\psi(4415)$  through electromagnetic transitions. For example,  $\psi(4415)$  E1 decays are predicted to produce 3P states with branching fractions at the per mil level. These states could then be identified through their subsequent open-charm strong decays.

As discussed in Section V.C, two new states near 3940 MeV have recently been reported by Belle.  $2P$   $\chi_J$  states are natural assignments, as they have theoretical quark model masses ranging from 3852 to 3972 MeV and widths of 50-100 MeV, similar to the reported values. A measurement of the relative branching fractions to DD,

DD\* and  $D^*D^*$  and comparisons to our  $^3P_0$  decay model predictions should allow the determination of the quantum numbers of these states, and will show whether they are indeed consistent with  $2P$   $c\bar{c}$  assignments.

A better determination of the properties of conventional charmonium states at higher masses is important not only because of the improved understanding of QCD that will follow (especially aspects of confinement and strong decays), but also because qualitatively different types of resonances are expected at these masses. These new states include charmed meson molecules and charmonium hybrids, and the identification of these novel excitations will obviously be easier if the conventional charmonium spectrum is well established.

The recent results from B factories and new programs at BES, CLEO and GSI have led to a resurgence of interest in the physics of charmonium. We argue that a detailed experimental investigation of the spectrum of excited charmonium states and their decay properties will considerably improve our understanding of the nonperturbative aspects of QCD.

#### Acknowledgments

We acknowledge useful discussions with R.Galik, T.Pedlar, C.Quigg, J.Rosner, K.Seth and T.Swarnicki in the course of this work.

This research was supported in part by the Natural Sciences and Engineering Research Council of Canada, the U.S. National Science Foundation through grant NSF-PHY-0244786 at the University of Tennessee, and the U.S. Department of Energy under contracts DE-AC05-00OR22725 at Oak Ridge National Laboratory and DE-FG02-00ER41135 at the University of Pittsburgh, and by PPARC grant PP/B500607.

- 
- [1] J. J. Aubert *et al.* [E598 Collaboration], Phys. Rev. Lett. **33**, 1404 (1974).
  - [2] J. E. Augustin *et al.* [SLAC-SP-017 Collaboration], Phys. Rev. Lett. **33**, 1406 (1974).
  - [3] T. Appelquist and H. D. Politzer, Phys. Rev. Lett. **34**, 43 (1975).
  - [4] A. De Rujula and S. L. Glashow, Phys. Rev. Lett. **34**, 46 (1975).
  - [5] T. Appelquist, A. De Rujula, H. D. Politzer and S. L. Glashow, Phys. Rev. Lett. **34**, 365 (1975).
  - [6] E. Eichten, K. Gottfried, T. Kinoshita, J. B. Kogut, K. D. Lane and T. M. Yan, Phys. Rev. Lett. **34**, 369 (1975) [Erratum-ibid. **36**, 1276 (1976)].
  - [7] C. Quigg, arXiv:hep-ph/0403187.
  - [8] R. S. Galik, arXiv:hep-ph/0408190.
  - [9] N. Brambilla *et al.*, arXiv:hep-ph/0412158.
  - [10] K. K. Seth, arXiv:hep-ex/0501022. This reference in effect quotes a combined average mass for the  $h_c$  of  $3524.65 \pm 0.55$  MeV from new CLEO measurements.
  - [11] K. K. Seth, arXiv:hep-ex/0504050.
  - [12] K. K. Seth, arXiv:hep-ex/0504052.
  - [13] T. Skwarnicki, arXiv:hep-ex/0505050.
  - [14] E.J.Eichten, K.Lane and C.Quigg, Phys. Rev. Lett. **89**, 162002 (2002) [arXiv:hep-ph/0206018].
  - [15] The BESIII Detector. Preliminary Design Report, IHEP-BEPCH-SB-13 (Jan. 2004).
  - [16] R. A. Briere *et al.*, "CLEO-c and CESR-c: A New Frontier of Weak and Strong Interactions", CLNS 01/1742 (Oct. 2001).
  - [17] Technical Progress Report for PANDA. Strong Interaction Studies with Antiprotons. (PANDA Collaboration, Feb. 2005); available at [http://www.ep1.rub.de/~panda/archive/public/panda\\_tpr.pdf](http://www.ep1.rub.de/~panda/archive/public/panda_tpr.pdf)
  - [18] S.-K.Choi *et al.* (Belle Collaboration), Phys. Rev. Lett. **89**, 102001 (2002), err. ibid. **89**, 129901 (2002). [arXiv:hep-ex/0206002].
  - [19] B. Aubert *et al.* [BABAR Collaboration], Phys. Rev. Lett. **92**, 142002 (2004) [arXiv:hep-ex/0311038].
  - [20] D.M.Asner *et al.* (CLEO Collaboration), Phys. Rev. Lett.**92**, 142001 (2004) [arXiv:hep-ex/0312058].
  - [21] S. K. Choi *et al.* [Belle Collaboration], Phys. Rev. Lett.

TABLE I: Experimental and theoretical spectrum of  $c\bar{c}$  states. The experimental masses are PDG averages, which are rounded to 1 MeV and assigned equal weights in the theoretical fits. For the  $2^1S_0$   $\eta'_c(3638)$  we use a world average of recent measurements [86].

Multiplet	State	Expt.	Input (NR)	Theor.	
				NR	GI
1S	$J/\psi(1^3S_1)$	$3096.87 \pm 0.04$	3097	3090	3098
	$\eta_c(1^1S_0)$	$2979.2 \pm 1.3$	2979	2982	2975
2S	$\psi'(2^3S_1)$	$3685.96 \pm 0.09$	3686	3672	3676
	$\eta'_c(2^1S_0)$	$3637.7 \pm 4.4$	3638	3630	3623
3S	$\psi(3^3S_1)$	$4040 \pm 10$	4040	4072	4100
	$\eta_c(3^1S_0)$			4043	4064
4S	$\psi(4^3S_1)$	$4415 \pm 6$	4415	4406	4450
	$\eta_c(4^1S_0)$			4384	4425
1P	$\chi_2(1^3P_2)$	$3556.18 \pm 0.13$	3556	3556	3550
	$\chi_1(1^3P_1)$	$3510.51 \pm 0.12$	3511	3505	3510
	$\chi_0(1^3P_0)$	$3415.3 \pm 0.4$	3415	3424	3445
	$h_c(1^1P_1)$	see text		3516	3517
2P	$\chi_2(2^3P_2)$			3972	3979
	$\chi_1(2^3P_1)$			3925	3953
	$\chi_0(2^3P_0)$			3852	3916
	$h_c(2^1P_1)$			3934	3956
3P	$\chi_2(3^3P_2)$			4317	4337
	$\chi_1(3^3P_1)$			4271	4317
	$\chi_0(3^3P_0)$			4202	4292
	$h_c(3^1P_1)$			4279	4318
1D	$\psi_3(1^3D_3)$			3806	3849
	$\psi_2(1^3D_2)$			3800	3838
	$\psi(1^3D_1)$	$3769.9 \pm 2.5$	3770	3785	3819
	$\eta_{c2}(1^1D_2)$			3799	3837
2D	$\psi_3(2^3D_3)$			4167	4217
	$\psi_2(2^3D_2)$			4158	4208
	$\psi(2^3D_1)$	$4159 \pm 20$	4159	4142	4194
	$\eta_{c2}(2^1D_2)$			4158	4208
1F	$\chi_4(1^3F_4)$			4021	4095
	$\chi_3(1^3F_3)$			4029	4097
	$\chi_2(1^3F_2)$			4029	4092
	$h_{c3}(1^1F_3)$			4026	4094
2F	$\chi_4(2^3F_4)$			4348	4425
	$\chi_3(2^3F_3)$			4352	4426
	$\chi_2(2^3F_2)$			4351	4422
	$h_{c3}(2^1F_3)$			4350	4424
1G	$\psi_5(1^3G_5)$			4214	4312
	$\psi_4(1^3G_4)$			4228	4320
	$\psi_3(1^3G_3)$			4237	4323
	$\eta_{c4}(1^1G_4)$			4225	4317

- 91, 262001 (2003) [arXiv:hep-ex/0309032].
- [22] D. Acosta *et al.* [CDF II Collaboration], Phys. Rev. Lett. 93, 072001 (2004) [arXiv:hep-ex/0312021].
- [23] F. E. Close and P. R. Page, Phys. Lett. B578, 119 (2004) [arXiv:hep-ph/0309253].
- [24] E. S. Swanson, Phys. Lett. B588, 189 (2004) [arXiv:hep-ph/0311229].
- [25] N. A. Tornqvist, Phys. Lett. B **590**, 209 (2004) [arXiv:hep-ph/0402237].
- [26] T. Barnes and S. Godfrey, Phys. Rev. D69, 054008 (2004) [arXiv:hep-ph/0311162].
- [27] E. J. Eichten, K. Lane and C. Quigg, Phys. Rev. D69, 094019 (2004) [arXiv:hep-ph/0401210].
- [28] K. Abe, arXiv:hep-ex/0505037.
- [29] K. Abe, arXiv:hep-ex/0505038.
- [30] A. Tomaradze, J. Phys. Conf. Ser. **9**, 119 (2005) [arXiv:hep-ex/0410090]. The reported  $h_c$  signal is in the decay chain  $\psi' \rightarrow \pi^0 h_c$ ,  $h_c \rightarrow \gamma \eta_c$ . The masses found in two different inclusive analyses were  $3524.8 \pm 0.7$  MeV and  $3524.8 \pm 0.7$  MeV (with an estimated systematic error of  $\sim 1$  MeV, and  $3524.4 \pm 0.9$  MeV in exclusive decays (with six different identified  $\eta_c$  final states).
- [31] K. Abe *et al.* [Belle Collaboration], Phys. Rev. Lett. 89, 142001 (2002) [arXiv:hep-ex/0205104].

TABLE II:  $S \rightarrow P$  E1 radiative transitions in the NR and GI potential models. The masses are taken from Table I; we use the experimental masses (rounded “input” column) if known, and for the  $^1P_1$   $h_c$  we assume a mass of 3525 MeV, which is the c.o.g. of the  $^3P_J$   $\chi_J$  states. Otherwise, theoretical values are used.

Multiplets	Initial meson	Final meson	$E_\gamma$ (MeV)		$\Gamma_{\text{thy}}$ (keV)		$\Gamma_{\text{expt}}$ (keV)
			NR	GI	NR	GI	
2S $\rightarrow$ 1P	$\psi'(2^3S_1)$	$\chi_2(1^3P_2)$	128.	128.	38.	24.	$27. \pm 4.$
		$\chi_1(1^3P_1)$	171.	171.	54.	29.	$27. \pm 3.$
		$\chi_0(1^3P_0)$	261.	261.	63.	26.	$27. \pm 3.$
	$\eta'_c(2^1S_0)$	$h_c(1^1P_1)$	111.	119.	49.	36.	
3S $\rightarrow$ 2P	$\psi(3^3S_1)$	$\chi_2(2^3P_2)$	67.	119.	14.	48.	
		$\chi_1(2^3P_1)$	113.	145.	39.	43.	
		$\chi_0(2^3P_0)$	184.	180.	54.	22.	
	$\eta_c(3^1S_0)$	$h_c(2^1P_1)$	108.	108.	105.	64.	
3S $\rightarrow$ 1P	$\psi(3^3S_1)$	$\chi_2(1^3P_2)$	455.	508.	0.70	12.7	
		$\chi_1(1^3P_1)$	494.	547.	0.53	0.85	
		$\chi_0(1^3P_0)$	577.	628.	0.27	0.63	
	$\eta_c(3^1S_0)$	$h_c(1^1P_1)$	485.	511.	9.1	28.	
4S $\rightarrow$ 3P	$\psi(4^3S_1)$	$\chi_2(3^3P_2)$	97.	112.	68.	66.	
		$\chi_1(3^3P_1)$	142.	131.	126.	54.	
		$\chi_0(3^3P_0)$	208.	155.	0.003	25.	
	$\eta_c(4^1S_0)$	$h_c(3^1P_1)$	104.	106.	159.	101.	
4S $\rightarrow$ 2P	$\psi(4^3S_1)$	$\chi_2(2^3P_2)$	421.	446.	0.62	15.	
		$\chi_1(2^3P_1)$	423.	469.	0.49	0.92	
		$\chi_0(2^3P_0)$	527.	502.	0.24	0.39	
	$\eta_c(4^1S_0)$	$h_c(2^1P_1)$	427.	444.	10.1	31.3	
4S $\rightarrow$ 1P	$\psi(4^3S_1)$	$\chi_2(^3P_2)$	775.	804.	0.61	5.2	
		$\chi_1(^3P_1)$	811.	841.	0.41	0.53	
		$\chi_0(^3P_0)$	887.	915.	0.18	0.13	
	$\eta_c(4^1S_0)$	$h_c(^1P_1)$	782.	808.	5.2	9.6	

TABLE III: 1P and 2P E1 radiative transitions (format as in Table II).

Multiplets	Initial meson	Final meson	$E_\gamma$ (MeV)		$\Gamma_{\text{thy}}$ (keV)		$\Gamma_{\text{expt}}$ (keV)
			NR	GI	NR	GI	
1P $\rightarrow$ 1S	$\chi_2(1^3P_2)$	$J/\psi(1^3S_1)$	429.	429.	424.	313.	426. $\pm$ 51.
	$\chi_1(1^3P_1)$		390.	389.	314.	239.	291. $\pm$ 48.
	$\chi_0(1^3P_0)$		303.	303.	152.	114.	119. $\pm$ 19.
	$h_c(1^1P_1)$	$\eta_c(1^1S_0)$	504.	496.	498.	352.	
2P $\rightarrow$ 2S	$\chi_2(2^3P_2)$	$\psi'(2^3S_1)$	276.	282.	304.	207.	
	$\chi_1(2^3P_1)$		232.	258.	183.	183.	
	$\chi_0(2^3P_0)$		162.	223.	64.	135.	
	$h_c(2^1P_1)$	$\eta'_c(2^1S_0)$	285.	305.	280.	218.	
2P $\rightarrow$ 1S	$\chi_2(2^3P_2)$	$J/\psi(1^3S_1)$	779.	784.	81.	53.	
	$\chi_1(2^3P_1)$		741.	763.	71.	14.	
	$\chi_0(2^3P_0)$		681.	733.	56.	1.3	
	$h_c(2^1P_1)$	$\eta_c(1^1S_0)$	839.	856.	140.	85.	
2P $\rightarrow$ 1D	$\chi_2(2^3P_2)$	$\psi_3(1^3D_3)$	163.	128.	88.	29.	
		$\psi_2(1^3D_2)$	168.	139.	17.	5.6	
		$\psi(1^3D_1)$	197.	204.	1.9	1.0	
	$\chi_1(2^3P_1)$	$\psi_2(1^3D_2)$	123.	113.	35.	18.	
		$\psi(1^3D_1)$	152.	179.	22.	21.	
	$\chi_0(2^3P_0)$	$\psi(1^3D_1)$	81.	143.	13.	51.	
	$h_c(2^1P_1)$	$\eta_{2c}(1^1D_2)$	133.	117.	60.	27.	

- [32] K. Abe *et al.* [Belle Collaboration], Phys. Rev. D **70**, 071102 (2004) [arXiv:hep-ex/0407009].
- [33] P. Pakhlov, [arXiv:hep-ex/0412041].
- [34] P. Pakhlov (private communication).
- [35] E. Eichten, K. Gottfried, T. Kinoshita, K. D. Lane and T. M. Yan, Phys. Rev. D **17**, 3090 (1978) [Erratum-ibid. D **21**, 313 (1980)].
- [36] D. Ebert, R. N. Faustov and V. O. Galkin, arXiv:hep-ph/0503012.
- [37] C. W. Bernard *et al.* [MILC Collaboration], Phys. Rev. D **56**, 7039 (1997) [arXiv:hep-lat/9707008].
- [38] X. Liao and T. Manke, [arXiv:hep-lat/0210030].
- [39] Z. H. Mei and X. Q. Luo, Int. J. Mod. Phys. A **18**, 5713 (2003) [arXiv:hep-lat/0206012].
- [40] G. S. Bali, Eur. Phys. J. A **19**, 1 (2004) [arXiv:hep-lat/0308015].
- [41] B. Aubert *et al.* [BABAR Collaboration], Phys. Rev. Lett. **90**, 242001 (2003) [arXiv:hep-ex/0304021].
- [42] D. Besson *et al.* [CLEO Collaboration], AIP Conf. Proc. **698**, 497 (2004) [arXiv:hep-ex/0305017].
- [43] E. S. Swanson, Phys. Lett. B **582**, 167 (2004) [arXiv:hep-ph/0309296].
- [44] D. Ebert, R. N. Faustov and V. O. Galkin, Phys. Rev. D **67**, 014027 (2003) [arXiv:hep-ph/0210381].
- [45] T. Barnes, [arXiv:hep-ph/0406327].
- [46] Z. P. Li, F. E. Close and T. Barnes, Phys. Rev. D **43**,

TABLE IV: 3P E1 radiative transitions (format as in Table II).

Multiplets	Initial meson	Final meson	$E_\gamma$ (MeV)		$\Gamma_{\text{thy}}$ (keV)		$\Gamma_{\text{expt}}$ (keV)
			NR	GI	NR	GI	
3P $\rightarrow$ 3S	$\chi_2(3^3P_2)$	$\psi(3^3S_1)$	268.	231.	509.	199.	
	$\chi_1(3^3P_1)$		225.	212.	303.	181.	
	$\chi_0(3^3P_0)$		159.	188.	109.	145.	
	$h_c(3^1P_1)$	$\eta_c(3^1S_0)$	229.	246.	276.	208.	
3P $\rightarrow$ 2S	$\chi_2(3^3P_2)$	$\psi'(2^3S_1)$	585.	602.	55.	30.	
	$\chi_1(3^3P_1)$		545.	585.	45.	8.9	
	$\chi_0(3^3P_0)$		484.	563.	32.	0.045	
	$h_c(3^1P_1)$	$\eta'_c(2^1S_0)$	593.	627.	75.	43.	
3P $\rightarrow$ 1S	$\chi_2(3^3P_2)$	$J/\psi(1^3S_1)$	1048.	1063.	34.	19.	
	$\chi_1(3^3P_1)$		1013.	1048.	31.	2.2	
	$\chi_0(3^3P_0)$		960.	1029.	27.	1.5	
	$h_c(3^1P_1)$	$\eta_c(1^1S_0)$	1103.	1131.	72.	38.	
3P $\rightarrow$ 2D	$\chi_2(3^3P_2)$	$\psi_3(2^3D_3)$	147.	118.	148.	51.	
		$\psi_2(2^3D_2)$	156.	127.	31.	9.9	
		$\psi(2^3D_1)$	155.	141.	2.1	0.77	
	$\chi_1(3^3P_1)$	$\psi_2(2^3D_2)$	112.	108.	58.	35.	
		$\psi(2^3D_1)$	111.	121.	19.	15.	
	$\chi_0(3^3P_0)$	$\psi(2^3D_1)$	43.	97.	4.4	35.	
	$h_c(3^1P_1)$	$\eta_{2c}(2^1D_2)$	119.	109.	99.	48.	
3P $\rightarrow$ 1D	$\chi_2(3^3P_2)$	$\psi_3(1^3D_3)$	481.	461.	0.049	6.8	
		$\psi_2(1^3D_2)$	486.	470.	0.0091	0.13	
		$\psi(1^3D_1)$	512.	530.	0.00071	0.001	
	$\chi_1(3^3P_1)$	$\psi_2(1^3D_2)$	445.	452.	0.035	4.6	
		$\psi(1^3D_1)$	472.	512.	0.014	0.39	
	$\chi_0(3^3P_0)$	$\psi(1^3D_1)$	410.	490.	0.037	9.7	
	$h_c(3^1P_1)$	$\eta_{2c}(1^1D_2)$	453.	454.	0.16	5.7	



TABLE V: 1D and 2D E1 radiative transitions (format as in Table II).

Multiplets	Initial meson	Final meson	$E_\gamma$ (MeV)		$\Gamma_{\text{thy}}$ (keV)		$\Gamma_{\text{expt}}$ (keV)
			NR	GI	NR	GI	
1D $\rightarrow$ 1P	$\psi_3(1^3D_3)$	$\chi_2(1^3P_2)$	242.	282.	272.	296.	
	$\psi_2(1^3D_2)$	$\chi_2(1^3P_2)$	236.	272.	64.	66.	
		$\chi_1(1^3P_1)$	278.	314.	307.	268.	
	$\psi(1^3D_1)$	$\chi_2(1^3P_2)$	208.	208.	4.9	3.3	$\leq 330$ (90% <i>c.l.</i> ) [76, 87]
		$\chi_1(1^3P_1)$	250.	251.	125.	77.	$280 \pm 100$ [76, 87]
		$\chi_0(1^3P_0)$	338.	338.	403.	213.	$320 \pm 120$ [76, 87]
	$h_{c2}(1^1D_2)$	$h_c(1^1P_1)$	264.	307.	339.	344.	
2D $\rightarrow$ 2P	$\psi_3(2^3D_3)$	$\chi_2(2^3P_2)$	190.	231.	239.	272.	
	$\psi_2(2^3D_2)$	$\chi_2(2^3P_2)$	182.	223.	52.	65.	
		$\chi_1(2^3P_1)$	226.	247.	298.	225.	
	$\psi(2^3D_1)$	$\chi_2(2^3P_2)$	183.	210.	5.9	6.3	
		$\chi_1(2^3P_1)$	227.	234.	168.	114.	
		$\chi_0(2^3P_0)$	296.	269.	483.	191.	
	$\eta_{c2}(2^1D_2)$	$h_c(2^1P_1)$	218.	244.	336.	296.	
2D $\rightarrow$ 1P	$\psi_3(2^3D_3)$	$\chi_2(1^3P_2)$	566.	609.	29.	16.	
	$\psi_2(2^3D_2)$	$\chi_2(1^3P_2)$	558.	602.	7.1	0.62	
		$\chi_1(1^3P_1)$	597.	640.	26.	23.	
	$\psi(2^3D_1)$	$\chi_2(1^3P_2)$	559.	590.	0.79	0.027	
		$\chi_1(1^3P_1)$	598.	628.	14.	3.4	
		$\chi_0(1^3P_0)$	677.	707.	27.	35.	
	$h_{c2}(2^1D_2)$	$h_c(1^1P_1)$	585.	634.	40.	25.	
2D $\rightarrow$ 1F	$\psi_3(2^3D_3)$	$\chi_4(1^3F_4)$	143.	120.	66.	26.	
		$\chi_3(1^3F_3)$	136.	114.	4.8	1.9	
		$\chi_2(1^3F_2)$	136.	123.	14.	0.055	
	$\psi_2(2^3D_2)$	$\chi_3(1^3F_3)$	127.	110.	44.	19.	
		$\chi_2(1^3F_2)$	127.	114.	5.6	2.4	
	$\psi(2^3D_1)$	$\chi_2(1^3F_2)$	128.	101.	51.	17.	
	$\eta_{c2}(2^1D_2)$	$h_{c3}(1^1F_3)$	130.	112.	54.	23.	

TABLE VI: 1F E1 radiative transitions (format as in Table II).

Multiplets	Initial meson	Final meson	$E_\gamma$ (MeV)		$\Gamma_{\text{thy}}$ (keV)		$\Gamma_{\text{expt}}$ (keV)
			NR	GI	NR	GI	
1F $\rightarrow$ 1D	$\chi_4(1^3F_4)$	$\psi_3(1^3D_3)$	209.	239.	332.	334.	
	$\chi_3(1^3F_3)$	$\psi_3(1^3D_3)$	217.	240.	41.	38.	
		$\psi_2(1^3D_2)$	222.	251.	354.	325.	
	$\chi_2(1^3F_2)$	$\psi_3(1^3D_3)$	217.	236.	1.6	1.4	
		$\psi_2(1^3D_2)$	222.	246.	62.	69.	
		$\psi(1^3D_1)$	251.	309.	475.	541.	
	$h_{c3}(1^1F_3)$	$\eta_{c2}(1^1D_2)$	221.	249.	387.	321.	

- 2161 (1991).
- [47] E. S. Ackleh and T. Barnes, Phys. Rev. D **45**, 232 (1992).
- [48] E. S. Ackleh, T. Barnes and F. E. Close, Phys. Rev. D **46**, 2257 (1992).
- [49] T. Barnes and G. I. Ghandour, Phys. Lett. B118, 411 (1982).
- [50] S. Godfrey and N. Isgur, Phys. Rev. D32, 189 (1985).
- [51] M. Okamoto *et al.* [CP-PACS Collaboration], Phys. Rev. D **65**, 094508 (2002) [arXiv:hep-lat/0112020].
- [52] S. Hashimoto and T. Onogi, Ann. Rev. Nucl. Part. Sci. **54**, 451 (2004) [arXiv:hep-ph/0407221].
- [53] W. Kwong and J. L. Rosner, Phys. Rev. D38, 279 (1988).
- [54] L. Micu, Nucl. Phys. B10, 521 (1969).
- [55] A. Le Yaouanc, L. Oliver, O. Pène and J.-C. Raynal, Phys. Rev. D8, (1973) 2223.
- [56] A. Le Yaouanc, L. Oliver, O. Pène and J.-C. Raynal, Phys. Rev. D9, 1415 (1974).
- [57] A. Le Yaouanc, O. Pène, J.-C. Raynal and L. Oliver, Nucl. Phys. B149, 321 (1979).
- [58] A. Le Yaouanc, L. Oliver, O. Pène and J.-C. Raynal, Phys. Lett. B71, 397 (1977).
- [59] A. Le Yaouanc, L. Oliver, O. Pène and J.-C. Raynal, Phys. Lett. B72, 57 (1977).
- [60] R. Kokoski and N. Isgur, Phys. Rev. D35, 907 (1987).
- [61] E. S. Ackleh, T. Barnes and E. S. Swanson, Phys. Rev. D54, 6811 (1996). [arXiv:hep-ph/9604355].
- [62] M. Nozar *et al.* [E852 Collaboration], Phys. Lett. B541, 35 (2002) [arXiv:hep-ex/0206026].
- [63] D. V. Amelin *et al.* [VES Collaboration], [arXiv:hep-ex/9810013].
- [64] S. Eidelman *et al.* (Particle Data Group), Phys. Lett. B592, 1 (2004).
- [65] W. Roberts and B. Silvestre-Brac, Phys. Rev. D57, 1694 (1998). [arXiv:hep-ph/9708235].
- [66] T. Barnes, F. E. Close, P. R. Page and E. S. Swanson, Phys. Rev. D55, 4157 (1997). [arXiv:hep-ph/9609339].
- [67] T. Barnes, N. Black and P. R. Page, Phys. Rev. D68, 054014 (2003) [arXiv:nucl-th/0208072].
- [68] F. E. Close and P. R. Page, Phys. Lett. B **366**, 323 (1996) [arXiv:hep-ph/9507407].
- [69] P. Geiger and E. S. Swanson, Phys. Rev. D50, 6855 (1994) [arXiv:hep-ph/9405238].
- [70] H. G. Blundell and S. Godfrey, Phys. Rev. D53, 3700 (1996) [arXiv:hep-ph/9508264].
- [71] K. Abe *et al.* [Belle Collaboration], Phys. Rev. D69, 112002 (2004) [arXiv:hep-ex/0307021].
- [72] E. W. Vaandering [FOCUS Collaboration], [arXiv:hep-ex/0406044].
- [73] R. Kutschke, private communication.
- [74] S. Godfrey and R. Kokoski, Phys. Rev. D43, 1679 (1991).
- [75] J. L. Rosner, [arXiv:hep-ph/0411003].
- [76] J. L. Rosner, [arXiv:hep-ph/0405196].
- [77] G. Goldhaber *et al.*, Phys. Lett. B69, 503 (1977).
- [78] M. B. Voloshin and L. B. Okun, JETP Lett. 23, 333 (1976) [Pisma Zh. Eksp. Teor. Fiz. 3, 369 (1976)].
- [79] A. De Rújula, H. Georgi and S. L. Glashow, Phys. Rev. Lett. 38, 317 (1977).
- [80] S. Iwao, Lett. Nuovo Cim. 28, 305 (1980).
- [81] K. K. Seth, [arXiv:hep-ex/0405007].
- [82] N. Isgur, R. Kokoski and J. Paton, Phys. Rev. Lett. 54, 869 (1985).
- [83] J. M. Link *et al.* [FOCUS Collaboration], Phys. Lett. B586, 11 (2004) [arXiv:hep-ex/0312060].
- [84] P. S. Cooper, "New Results in Charm Meson Spectroscopy from FOCUS and SELEX", presented at GHP2004 (Fermilab, 24-26 Oct 2004).
- [85] K. Abe *et al.* [Belle Collaboration], [arXiv:hep-ex/0408126].
- [86] T. Skwarnicki, Int J. Mod. Phys. A **19**, 1030 (2004).
- [87] Y. Zhu, Ph.D. Thesis, California Institute of Technology, 1988, Caltech report CALT-68-1513 (unpublished).

TABLE VII: 2F E1 radiative transitions (format as in Table II).

Multiplets	Initial meson	Final meson	$E_\gamma$ (MeV)		$\Gamma_{\text{thy}}$ (keV)		$\Gamma_{\text{expt}}$ (keV)
			NR	GI	NR	GI	
2F $\rightarrow$ 2D	$\chi_4(2^3F_4)$	$\psi_3(2^3D_3)$	177.	203.	307.	297.	
	$\chi_3(2^3F_3)$	$\psi_3(2^3D_3)$	181.	204.	36.	35.	
		$\psi_2(2^3D_2)$	190.	213.	334.	289.	
		$\psi_3(2^3D_3)$	180.	200.	1.4	1.4	
	$\chi_2(2^3F_2)$	$\psi_2(2^3D_2)$	189.	209.	58.	50.	
		$\psi(2^3D_1)$	188.	222.	306.	295.	
		$\eta_{c2}(2^1D_2)$	188.	211.	362.	284.	
2F $\rightarrow$ 1D	$\chi_4(2^3F_4)$	$\psi_3(1^3D_3)$	508.	539.	20.	8.6	
	$\chi_3(2^3F_3)$	$\psi_3(1^3D_3)$	512.	539.	2.3	0.14	
		$\psi_2(1^3D_2)$	517.	549.	19.	11.	
		$\psi_3(1^3D_3)$	511.	536.	0.090	0.003	
	$\chi_2(2^3F_2)$	$\psi_2(1^3D_2)$	516.	545.	3.2	0.39	
		$\psi(1^3D_1)$	542.	604.	20.	18.	
		$\eta_{c2}(2^1F_3)$	$\eta_{c2}(1^1D_2)$	516.	548.	22.	9.9
2F $\rightarrow$ 1G	$\chi_4(2^3F_4)$	$\psi_5(1^3G_5)$	132.	112.	54.	22.	
		$\psi_4(1^3G_4)$	118.	104.	2.0	0.84	
		$\psi_3(1^3G_3)$	110.	101.	0.025	0.011	
	$\chi_3(2^3F_3)$	$\psi_4(1^3G_4)$	122.	105.	43.	18.	
		$\psi_3(1^3G_3)$	113.	102.	2.3	1.0	
		$\psi_3(1^3G_3)$	113.	98.	36.	16.	
	$\chi_2(2^3F_2)$	$\eta_{c4}(2^1F_3)$	$\eta_{c4}(1^1G_4)$	123.	106.	47.	20.

TABLE VIII: 1G E1 radiative transitions (format as in Table II).

Multiplets	Initial meson	Final meson	$E_\gamma$ (MeV)		$\Gamma_{\text{thy}}$ (keV)		$\Gamma_{\text{expt}}$ (keV)
			NR	GI	NR	GI	
1G $\rightarrow$ 1F	$\psi_5(1^3G_5)$	$\chi_4(1^3F_4)$	189.	212.	373.	355.	
	$\psi_4(1^3G_4)$	$\chi_4(1^3F_4)$	202.	219.	29.	25.	
		$\chi_3(1^3F_3)$	194.	217.	382.	349.	
	$\psi_3(1^3G_3)$	$\chi_4(1^3F_4)$	210.	222.	0.66	0.52	
		$\chi_3(1^3F_3)$	203.	220.	37.	31.	
		$\chi_2(1^3F_2)$	203.	225.	425.	366.	
	$\eta_{c4}(1^1G_4)$	$h_{c3}(1^1F_3)$	194.	217.	407.	374.	

TABLE IX: M1 radiative partial widths. The assumed masses are experimental where known, and otherwise are the theoretical predictions (see Table I). One exception is the  $\eta_c(3^1S_0)$ , for which we assume a mass of 4011 MeV (the mass of the known  $\psi(4040)$  minus the theoretical 3S splitting). We give results for the NR model (both with and without the recoil factor of  $j_0(kr/2)$ ) and the GI model, which includes the recoil factor.

Initial Multiplet	Initial meson	Final meson	$E_\gamma$ (MeV)		$\Gamma_{\text{thy}}$ (keV)			$\Gamma_{\text{expt}}$ (keV)
			NR	GI	NR	NR( $j_0$ )	GI	
1S	$J/\psi(1^3S_1)$	$\eta_c(1^1S_0)$	116.	115.	2.9	2.9	2.4	$1.1 \pm 0.3$
2S	$\psi'(2^3S_1)$	$\eta'_c(2^1S_0)$	48.	48.	0.21	0.21	0.17	
		$\eta_c(1^1S_0)$	639.	638.	4.6	9.7	9.6	$0.8 \pm 0.2$
	$\eta'_c(2^1S_0)$	$J/\psi(1^3S_1)$	501.	501.	7.9	2.5	5.6	
3S	$\psi(3^3S_1)$	$\eta_c(3^1S_0)$	29.	35.	0.046	0.046	0.067	
		$\eta'_c(2^1S_0)$	382.	436.	0.61	1.8	2.6	
		$\eta_c(1^1S_0)$	922.	967.	3.5	8.7	9.0	
	$\eta_c(3^1S_0)$	$\psi'(2^3S_1)$	312.	361.	1.3	0.22	0.84	
		$J/\psi(1^3S_1)$	810.	853.	6.3	1.9	6.9	
2P	$h'_c(2^1P_1)$	$\chi_2(1^3P_2)$	360.	380.	0.071	0.075	0.11	
		$\chi_1(1^3P_1)$	400.	420.	0.058	0.13	0.36	
		$\chi_0(1^3P_0)$	485.	504.	0.033	0.21	1.5	
	$\chi'_2(2^3P_2)$	$h_c(1^1P_1)$	430.	435.	0.067	0.90	1.3	
	$\chi'_1(2^3P_1)$	$h_c(1^1P_1)$	388.	412.	0.050	0.51	0.045	
	$\chi'_0(2^3P_0)$	$h_c(1^1P_1)$	321.	379.	0.029	0.19	0.50	

TABLE X: Open-flavor strong decays, 3S and 4S states. The  $\psi(4040)$  and  $\psi(4415)$  masses (boldface) are taken from experiment; for the remaining (unknown) masses we assume the theoretical NR potential model values of Table I.

Meson	State	Mode	$\Gamma_{thy}$ [ $\Gamma_{expt}$ ] (MeV)	Amps. ( $\text{GeV}^{-1/2}$ )	
$\psi(\mathbf{4040})$	$3^3S_1$	DD	0.1	$^1P_1 = -0.0052$	
		DD*	33	$^3P_1 = -0.0954$	
		D*D*	33	$^1P_1 = +0.0338$	
				$^5P_1 = -0.1510$	
				$^5F_1 = 0$	
		$D_s D_s$	7.8	$^1P_1 = +0.0518$	
		<i>total</i>	74 [52 ± 10]		
$\eta_c(4043)$	$3^1S_0$	DD*	47	$^3P_0 = -0.1139$	
		D*D*	33	$^3P_0 = -0.1489$	
		<i>total</i>	80		
$\psi(\mathbf{4415})$	$4^3S_1$	DD	0.4	$^1P_1 = +0.0066$	
		DD*	2.3	$^3P_1 = +0.0177$	
		D*D*	16	$^1P_1 = -0.0109$	
				$^5P_1 = +0.0487$	
				$^5F_1 = 0$	
			DD <sub>1</sub>	31	$^3S_1 = 0$
					$^3D_1 = +0.0933$
			DD' <sub>1</sub>	1.0	$^3S_1 = +0.0168$
					$^3D_1 = 0$
			DD <sub>2</sub> *	23	$^5D_1 = -0.0881$
			D*D <sub>0</sub> *	0.0	$^3S_1 = -8.7 \cdot 10^{-4}$
				0	$^3D_1 = 0$
			$D_s D_s$	1.3	$^1P_1 = -0.0135$
	$D_s D_s^*$	2.6	$^3P_1 = +0.0212$		
	$D_s^* D_s^*$	0.7	$^1P_1 = +0.0027$		
			$^5P_1 = -0.0119$		
			$^5F_1 = 0$		
		<i>total</i>	78 [43 ± 15]		
$\eta_c(4384)$	$4^1S_0$	DD*	6.3	$^3P_0 = +0.0299$	
		D*D*	14	$^3P_0 = +0.0473$	
		DD <sub>0</sub> *	11	$^1S_0 = +0.0497$	
		DD <sub>2</sub> *	24	$^5D_0 = -0.1014$	
		$D_s D_s^*$	2.2	$^3P_0 = +0.0201$	
		$D_s^* D_s^*$	2.2	$^3P_0 = -0.0231$	
		$D_s D_{s0}^*$	0.6	$^1S_0 = -0.0136$	
		<i>total</i>	61		

TABLE XI: Open-flavor strong decays, 2P and 3P states. The initial meson masses are predictions of the NR potential model, Table I.

Meson	State	Mode	$\Gamma_{thy}$ (MeV)	Amps. ( $\text{GeV}^{-1/2}$ )		
$\chi_2(3972)$	$2^3P_2$	DD	42	$^1D_2 = +0.0992$		
		DD*	37	$^3D_2 = -0.1172$		
		$D_s D_s$	0.7	$^1D_2 = +0.0202$		
		<i>total</i>	80			
$\chi_1(3925)$	$2^3P_1$	DD*	165	$^3S_1 = +0.2883$ $^3D_1 = -0.0525$		
$\chi_0(3852)$	$2^3P_0$	DD	30	$^1S_0 = +0.1025$		
$h_c(3934)$	$2^1P_1$	DD*	87	$^3S_1 = -0.1847$ $^3D_1 = -0.0851$		
$\chi_2(4317)$	$3^3P_2$	DD	8.0	$^1D_2 = -0.0330$		
		DD*	2.4	$^3D_2 = +0.0191$		
		$D^*D^*$	24	$^5S_2 = +0.0592$ $^1D_2 = +0.0107$ $^5D_2 = -0.0282$ $^5G_2 = 0$		
		$DD_1$	1.1	$^3P_2 = +0.0240$ $^3F_2 = +0.0105$		
		$DD'_1$	12	$^3P_2 = -0.0915$ $^3F_2 = 0$		
		$D_s D_s$	0.8	$^1D_2 = +0.0115$		
		$D_s D_s^*$	11	$^3D_2 = -0.0474$		
		$D_s^* D_s^*$	7.2	$^5S_2 = -0.0266$ $^1D_2 = +0.0145$ $^5D_2 = -0.0384$ $^5G_2 = 0$		
		<i>total</i>	66			
		$\chi_1(4271)$	$3^3P_1$	DD*	6.8	$^3S_1 = -0.0337$ $^3D_1 = +0.0011$
				$D^*D^*$	19	$^5D_1 = -0.0632$
				$DD_0^*$	0.1	$^1P_1 = -0.0062$
				$D_s D_s^*$	9.7	$^3S_1 = -0.0287$ $^3D_1 = -0.0385$
$D_s^* D_s^*$	2.7			$^5D_1 = -0.0356$		
<i>total</i>	39					
$\chi_0(4202)$	$3^3P_0$	DD	0.5	$^1S_0 = -0.0091$		
		$D^*D^*$	43	$^1S_0 = -0.0267$ $^5D_0 = -0.0997$		
		$D_s D_s$	6.8	$^1S_0 = -0.0374$		
		<i>total</i>	51			
$h_c(4279)$	$3^1P_1$	DD*	3.0	$^3S_1 = +0.0216$ $^3D_1 = +0.0048$		
		$D^*D^*$	22	$^3S_1 = +0.0456$ $^3D_1 = -0.0487$		
		$DD_0^*$	28	$^1P_1 = -0.0943$		
		$D_s D_s^*$	15	$^3S_1 = +0.0222$ $^3D_1 = -0.0539$		
		$D_s^* D_s^*$	7.5	$^3S_1 = -0.0464$ $^3D_1 = -0.0327$		
		<i>total</i>	75			

TABLE XII: Open-flavor strong decays, 1D and 2D states. The  $\psi(3770)$  and  $\psi(4159)$  masses (boldface) are taken from experiment; for the remaining (unknown) masses we assume the theoretical NR potential model values of Table I.

Meson	State	Mode	$\Gamma_{thy}$ [ $\Gamma_{expt}$ ] (MeV)	Amps. ( $\text{GeV}^{-1/2}$ )
$\psi_3(3806)$	$1^3D_3$	DD	0.5	$^1F_3 = +0.0150$
$\psi(\mathbf{3770})$	$1^3D_1$	DD	43 [23.6 $\pm$ 2.7]	$^1P_1 = +0.1668$
$\psi_3(4167)$	$2^3D_3$	DD	24	$^1F_3 = +0.0631$
		DD*	50	$^3F_3 = -0.0997$
		D*D*	67	$^5P_3 = -0.1249$
				$^1F_3 = +0.0218$
				$^5F_3 = -0.0478$
				$^5H_3 = 0$
				$^1F_3 = +0.0358$
		$^3F_3 = -0.0205$		
		$D_s D_s$	5.7	
		$D_s D_s^*$	1.2	
		<i>total</i>	148	
$\psi_2(4158)$	$2^3D_2$	DD*	34	$^3P_2 = +0.0121$
				$^3F_2 = -0.0822$
		D*D*	32	$^5P_2 = -0.0660$
				$^5F_2 = -0.0685$
		$D_s D_s^*$	26	$^3P_2 = +0.0983$
		$^3F_2 = -0.0149$		
		<i>total</i>	92	
$\psi(\mathbf{4159})$	$2^3D_1$	DD	16	$^1P_1 = -0.0522$
		DD*	0.4	$^3P_1 = +0.0085$
		D*D*	35	$^1P_1 = +0.0489$
				$^5P_1 = -0.0219$
				$^5F_1 = -0.0845$
				$^1P_1 = -0.0427$
		$D_s D_s$	8.0	$^3P_1 = +0.0733$
		$D_s D_s^*$	14	
		<i>total</i>	74 [78 $\pm$ 20]	
$\eta_{c2}(4158)$	$2^1D_2$	DD*	50	$^3P_2 = -0.0099$
				$^3F_2 = -0.1007$
		D*D*	43	$^3P_2 = -0.0933$
				$^3F_2 = -0.0593$
		$D_s D_s^*$	18	$^3P_2 = -0.0802$
		$^3F_2 = -0.0182$		
		<i>total</i>	111	



TABLE XIII: Open-flavor strong decays, 1F states. The initial meson masses are predictions of the NR potential model, Table I.

Meson	State	Mode	$\Gamma_{thy}$ (MeV)	Amps. ( $\text{GeV}^{-1/2}$ )
$\chi_4(4021)$	$1^3F_4$	DD	6.8	$^1G_4 = +0.0379$
		DD*	1.4	$^3G_4 = -0.0204$
		D*D*	0.05	$^5D_4 = -0.0092$
				$^1G_4 = +1.2 \cdot 10^{-5}$
				$^5G_4 = -2.3 \cdot 10^{-5}$
			$^5I_4 = 0$	
		$D_s D_s$	0.02	$^1G_4 = +0.0029$
		<i>total</i>	8.3	
$\chi_3(4029)$	$1^3F_3$	DD*	83	$^3D_3 = +0.1534$
		D*D*	0.2	$^3G_3 = -0.0197$
				$^5D_3 = -0.0136$
		<i>total</i>	84	$^5G_3 = -2.4 \cdot 10^{-4}$
$\chi_2(4029)$	$1^3F_2$	DD	98	$^1D_2 = +0.1430$
		DD*	57	$^3D_2 = +0.1283$
		D*D*	0.1	$^5S_2 = 0$
				$^1D_2 = +0.0080$
				$^5D_2 = -0.0061$
		$D_s D_s$	5.9	$^5G_2 = -3.1 \cdot 10^{-4}$
		<i>total</i>	161	$^1D_2 = +0.0464$
$h_{c3}(4026)$	$1^1F_3$	DD*	61	$^3D_3 = -0.1313$
		D*D*	0.1	$^3G_3 = -0.0220$
				$^3D_3 = -0.0129$
		<i>total</i>	61	$^3G_3 = -1.3 \cdot 10^{-4}$

TABLE XIV: Open-flavor strong decays, 2F states. The initial meson masses are predictions of the NR potential model, Table I.

Meson	State	Mode	$\Gamma_{thy}$ (MeV)	Amps. ( $\text{GeV}^{-1/2}$ )
$\chi_4(4348)$	$2^3F_4$	DD	12	$^1G_4 = +0.0395$
		DD*	31	$^3G_4 = -0.0679$
		D*D*	21	$^5D_4 = -0.0386$
				$^1G_4 = +0.0209$
				$^5G_4 = -0.0415$
				$^5I_4 = 0$
		DD <sub>1</sub>	0.5	$^3F_4 = +0.0082$
				$^3H_4 = +0.0015$
		DD' <sub>1</sub>	2.0	$^3F_4 = -0.0172$
				$^3H_4 = 0$
		DD <sub>2</sub> *	0.04	$^5F_4 = -0.0051$
				$^3H_4 = -1.1 \cdot 10^{-4}$
		D*D <sub>0</sub> *	0.06	$^3F_4 = -0.0058$
				$^3H_4 = 0$
		D <sub>s</sub> D <sub>s</sub>	5.0	$^1G_4 = +0.0283$
D <sub>s</sub> D <sub>s</sub> *	4.3	$^3G_4 = -0.0290$		
D <sub>s</sub> *D <sub>s</sub> *	11	$^5D_4 = -0.0562$		
		$^1G_4 = +0.0034$		
		$^5G_4 = -0.0068$		
		$^5I_4 = 0$		
	<i>total</i>	87		
$\chi_3(4352)$	$2^3F_3$	DD*	27	$^3D_3 = -0.0208$
				$^3G_3 = -0.0597$
		D*D*	27	$^5D_3 = -0.0212$
				$^5G_3 = -0.0656$
		DD <sub>0</sub> *	0.6	$^1F_3 = -0.0119$
		DD <sub>1</sub>	3.4	$^3F_3 = -0.0237$
		DD' <sub>1</sub>	1.3	$^3F_3 = -0.0147$
		DD <sub>2</sub> *	32	$^5P_3 = +0.1432$
				$^5F_3 = +0.0025$
				$^5H_3 = -1.9 \cdot 10^{-4}$
		D*D <sub>0</sub> *	0.2	$^3F_3 = -0.0091$
		D <sub>s</sub> D <sub>s</sub> *	13	$^3D_3 = +0.0434$
				$^3G_3 = -0.0260$
		D <sub>s</sub> *D <sub>s</sub> *	4.3	$^5D_3 = -0.0328$
				$^5G_3 = -0.0112$
D <sub>s</sub> D <sub>s0</sub> *	0.04	$^1F_3 = -0.0039$		
	<i>total</i>	110		
$\chi_2(4351)$	$2^3F_2$	DD	15	$^1D_2 = -0.0446$
		DD*	2.0	$^3D_2 = -0.0171$
		D*D*	41	$^5S_2 = 0$
				$^1D_2 = +0.0127$
				$^5D_2 = -0.0096$
				$^5G_2 = -0.0828$
		DD <sub>1</sub>	105	$^3P_2 = +0.2093$
				$^3F_2 = +0.0167$
		DD' <sub>1</sub>	0.3	$^3P_2 = 0$
				$^3F_2 = -0.0113$
		DD <sub>2</sub> *	5.5	$^5P_2 = +0.0592$
		D*D <sub>0</sub> *	0.2	$^3F_2 = +0.0064$
		D <sub>s</sub> D <sub>s</sub>	1.1	$^1D_2 = +0.0134$
		D <sub>s</sub> D <sub>s</sub> *	6.9	$^3D_2 = +0.0365$
		D <sub>s</sub> *D <sub>s</sub> *	2.7	$^5S_2 = 0$
		$^1D_2 = +0.0194$		
		$^5D_2 = -0.0146$		
		$^5G_2 = -0.0140$		
	<i>total</i>	180		

TABLE XIV: Open-flavor strong decays, 2F states (cont.).

Meson	State	Mode	$\Gamma_{thy}$ (MeV)	Amps. ( $\text{GeV}^{-1/2}$ )
$h_{c3}(4350)$	$2^1F_3$	DD*	34	$^3D_3 = +0.0173$ $^3G_3 = -0.0689$
		D*D*	24	$^3D_3 = -0.0267$ $^3G_3 = -0.0584$
		DD <sub>0</sub> *	11	$^1F_3 = -0.0516$
		DD <sub>1</sub>	0.02	$^3F_3 = -0.0026$
		DD <sub>1</sub> '	0.03	$^3F_3 = -0.0035$
		DD <sub>2</sub> *	22	$^5P_3 = -0.1209$ $^5F_3 = -0.0070$ $^5H_3 = -1.8 \cdot 10^{-4}$
		D*D <sub>0</sub> *	0.006	$^3F_3 = -0.0018$
		D <sub>s</sub> D <sub>s</sub> *	12	$^3D_3 = -0.0379$ $^3G_3 = -0.0297$
		D <sub>s</sub> *D <sub>s</sub> *	6.0	$^3D_3 = -0.0400$ $^3G_3 = -0.0098$
		D <sub>s</sub> D <sub>s0</sub> *	0.3	$^1F_3 = -0.0108$
		<i>total</i>	109	

TABLE XV: Open-flavor strong decays, 1G states. The initial meson masses are predictions of the NR potential model, Table I.

Meson	State	Mode	$\Gamma_{thy}$ (MeV)	Amps. ( $\text{GeV}^{-1/2}$ )
$\psi_5(4214)$	$1^3G_5$	DD	10	$^1H_5 = +0.0397$
		DD*	6.4	$^3H_5 = -0.0342$
		D*D*	41	$^5F_5 = -0.0982$
				$^1H_5 = +0.0045$
				$^5H_5 = -0.0083$
				$^5J_5 = 0$
				$^1H_5 = +0.0086$
$\psi_4(4228)$	$1^3G_4$	D <sub>s</sub> D <sub>s</sub>	0.4	$^3H_5 = -0.0027$
		D <sub>s</sub> D <sub>s</sub> *	0.0	
		<i>total</i>	58	
		DD*	88	$^3F_4 = +0.1209$
		D*D*	19	$^3H_4 = -0.0334$
		D <sub>s</sub> D <sub>s</sub> *	3.5	$^5F_4 = -0.0643$
		D <sub>s</sub> *D <sub>s</sub> *	0.0	$^5H_4 = -0.0153$
$\psi_3(4237)$	$1^3G_3$			$^3F_4 = +0.0307$
				$^3H_4 = -0.0031$
		<i>total</i>	111	$^5F_4 = -1.5 \cdot 10^{-4}$
		DD	63	$^5H_4 = -6.0 \cdot 10^{-7}$
		DD*	66	
		D*D*	13	$^1F_3 = +0.0974$
				$^3F_3 = +0.1077$
$\eta_{c4}(4225)$	$1^1G_4$	D <sub>s</sub> D <sub>s</sub>	10	$^1F_3 = +0.0358$
		D <sub>s</sub> D <sub>s</sub> *	3	$^5F_3 = -0.0326$
		D <sub>s</sub> *D <sub>s</sub> *	0.0	$^5H_3 = -0.0217$
		<i>total</i>	155	$^1F_3 = +0.0443$
		DD*	72	$^3F_3 = +0.0289$
		D*D*	24	$^1F_3 = +4.6 \cdot 10^{-4}$
		D <sub>s</sub> D <sub>s</sub> *	3	$^5F_3 = -4.2 \cdot 10^{-4}$
$\eta_{c4}(4225)$	$1^1G_4$	D <sub>s</sub> *D <sub>s</sub> *	0.0	$^5H_3 = -1.4 \cdot 10^{-5}$
		<i>total</i>	99	
		DD*	72	$^3F_4 = -0.1076$
		D*D*	24	$^3H_4 = -0.0367$
		D <sub>s</sub> D <sub>s</sub> *	3	$^3F_4 = -0.0732$
		D <sub>s</sub> *D <sub>s</sub> *	0.0	$^3H_4 = -0.0136$
		<i>total</i>	99	$^3F_4 = -0.0268$
$\eta_{c4}(4225)$	$1^1G_4$			$^3H_4 = -0.0033$
				$^3F_4 = -2.2 \cdot 10^{-5}$
				$^3H_4 = -1.7 \cdot 10^{-8}$